



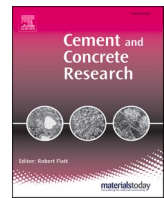
## **Long-term performance of reinforced concrete under a de-icing road environment**

Downloaded from: <https://research.chalmers.se>, 2025-05-17 12:25 UTC

Citation for the original published paper (version of record):

Tang, L., Boubitsas, D., Huang, L. (2023). Long-term performance of reinforced concrete under a de-icing road environment. *Cement and Concrete Research*, 164.  
<http://dx.doi.org/10.1016/j.cemconres.2022.107039>

N.B. When citing this work, cite the original published paper.



# Long-term performance of reinforced concrete under a de-icing road environment

Luping Tang<sup>a</sup>, Dimitrios Boubitsas<sup>b</sup>, Liming Huang<sup>a,c,\*</sup>

<sup>a</sup> Division of Building Technology, Chalmers University of Technology, 41296 Gothenburg, Sweden

<sup>b</sup> RISE Research Institute of Sweden, Braas, Sweden

<sup>c</sup> Key Laboratory of Advanced Civil Engineering Materials, Ministry of Education, Tongji University, Shanghai 201804, PR China

## ARTICLE INFO

### Keywords:

Chloride penetration  
De-icing salt  
Durability  
Field exposure  
Reinforcement corrosion

## ABSTRACT

In the middle of 1990, over 30 different mixes of concretes with eight different binders and water-binder ratios of 0.3 to 0.75 were exposed to a highway environment with a heavy de-icing salt spread for the examination of long-term performance, including chloride penetration, reinforcement corrosion and frost attack. This paper presents the results from this long-term study regarding chloride penetration and reinforcement corrosion. The results show that the chloride penetration in concretes under a de-icing salt road environment is much weaker than that in concretes under marine splash environment in Sweden. The estimated critical chloride content for the corrosion initiation is about 0.3 % by mass of binder for rebars with uncracked concrete cover. Considering the chloride redistribution in the surface zone, ClinConc model has been modified so that it can present a better description of the chloride profiles in the concretes at such an exposure site.

## 1. Introduction

The corrosion of reinforcing steel induced by chloride and frost damage are major challenges for the service life of reinforced concrete structures exposed to a de-icing salt environment. To design sustainable, economical, and safe concrete structures, models are needed for the description of chloride transport in concrete exposed to such an environment. Moreover, models are also significant to evaluate the residual service life for existing reinforced structures. They are applied to assess the starting time of reinforcement corrosion, internal frost damage or frost scaling. These models should be robust, credible, and based on the physical/chemical principle, which should also be validated with long-term results from the reinforced concrete structures installed in fields. The measured results can serve as input parameters in performance-based approach for offering rational designs, allowing innovation in concrete construction, and providing efficient means for assessing of the as-built structure [1].

Investigations of the frost resistance and corrosion of reinforcement steel induced by chloride have been initiated since the 1980's in Sweden. Many findings are well-known and popularly cited in current studies. These influential achievements include Tuutti's conceptual model for predicting service life of reinforced concretes [2], the slab-test for rating

the surface scaling [3] and internal damage [4] due to the frost attack, the frost and service life model by Fagerlund [5,6] and Petersson [7], the evaluation of the chloride penetration by the RCM (Rapid Chloride Migration) test [8,9], and the ClinConc model for predicting chloride penetration [9,10]. During the last decade, the ageing effect (hydration, drying and carbonation) on the salt-frost resistance of concrete was investigated by Utgenannt [11]. Fridh [12] performed experimental studies of the destruction mechanisms for the internal damages due to the frost attack. Tang and Utgenannt [13] reported the penetration of chloride into concrete after a 10-year exposure in the road environment. Li [14] carried out experimental investigations on the freeze-thaw induced chloride penetration into concretes. In the past years, Tang et al. [15] summarized different models for the prediction of resistance of chloride penetration into concrete and they also tried to use the field data to verify these models. Boubitsas et al. [16] reported the field data of chloride penetration into concretes with various binder types after an exposure of 20 years in a Swedish marine environment. Their findings regarding chloride penetration in concretes exposed to marine environments, especially those in the splash and atmospheric zones, could also be useful for understanding the chloride penetration in concretes under road environments exposed to de-icing salt due to the similarity in ageing processes.

\* Corresponding author at: Division of Building Technology, Chalmers University of Technology, 41296 Gothenburg, Sweden.

E-mail address: [limingh@chalmers.se](mailto:limingh@chalmers.se) (L. Huang).

<https://doi.org/10.1016/j.cemconres.2022.107039>

Received 24 April 2022; Received in revised form 1 November 2022; Accepted 19 November 2022

Available online 2 December 2022

0008-8846/© 2022 The Author(s). Published by Elsevier Ltd. This is an open access article under the CC BY license (<http://creativecommons.org/licenses/by/4.0/>).

Among the research in other countries, only a few literatures reported the corrosion resistance performance of the reinforced concrete under a de-icing salt environment. Polder and Hug [17] measured the penetration of chloride from de-icing salt in one bridge in Netherlands after a long-term service (30 years). Gode and Paeglitis [18] conducted an evaluation of the chloride migration in bridge piers under de-icing salt environment to predict the remaining service life. Some models were also developed to evaluate the chloride penetration under this environment with the consideration of carbonation [19] and cracking [20]. Although there are some ongoing projects in this area, problems still exist in the practical application of the experimental results in service life models for reinforced concrete structures under the road environments. It is mainly due to the lack of sufficient data from concrete with various binder types and proportions after a long-term exposure. An effective model for prediction of chloride penetration based on the field data is also needed under this special environment.

A series of reinforced concrete specimens have been exposed to de-icing salts at the field site by a highway Rv40 between Gothenburg and Borås in Sweden since the winter of 1996–1997. The severe cold weather in the winter needed an intensive use of de-icing salts on road for defrosting. Chloride penetration profiles in these concrete specimens were measured after an exposure for 1, 2, 5, 10, and 20 winters. Corrosion conditions of the embedded rebars in the specimens were examined after an exposure of 10 and 20 winters. These measured data

from exposure sites would function as the useful information about long-term performance of concretes served under the de-icing salts environment. With these data we can have the opportunity to validate various models for service life prediction. This paper presents the findings from this long-term study about the chloride penetration and corrosion of reinforcement. The ClinConc model [10] has been modified to present a better prediction of chloride penetration in concretes with different proportions after a long-term exposure to the de-icing road environment.

## 2. Experimental information

### 2.1. Concrete specimens

Concretes with 33 types of mixing proportion were designed for the long-term exposure experiments in the field site. The different mix proportions are presented in Table 1. The detailed information of the raw materials and properties of concrete were published in a previous report [21] and some fresh properties were presented in [22]. Concretes were cast with various water-binder ratios from 0.3 up to 0.75, and with eight types of binder system. Some concretes were added with air entraining agent (AEA) in a range of 0.008–0.04 % by mass of binder. Two types of concrete component were produced at the laboratory and then moved to the exposure site after a moist curing for 35 to 70 days in

**Table 1**  
Mixture proportions of concretes exposed at the Highway 40 field site.

Types of binder	w/b	Binder kg/m <sup>3</sup>	Fine kg/m <sup>3</sup>	Coarse kg/m <sup>3</sup>	AEA <sup>a</sup> mass %	Sp <sup>b</sup> mass %	Air vol%	28-day strength <sup>c</sup> MPa
Anl <sup>d</sup>	0.40	420	886.4	851.6	0.028	0.97	4.8	65.4
	0.50	380	890.2	821.8	0.012		4.5	50.8
	0.30	500	833.5	978.5		3.25	1.3	100.6
	0.35	450	880.3	953.7		2.27	0.9	91.3
	0.50	380	938.6	866.4			1.3	54.8
Anl + 5%SF <sup>e</sup>	0.75	260	1007.4	791.6	0.012		4.5	30
	0.40	420	860	860	0.04	1.2	4.7	78.1
	0.50	380	865.5	831.5	0.022		4.4	58.2
	0.30	500	806	985.1	0	1.7	1.2	119.7
	0.35	450	846.5	954.5	0	1.5	1.1	103.5
Fin Std <sup>f</sup>	0.50	380	905.8	870.2	0	0	0.9	62.6
	0.40	420	863	863	0.02	1.2	4.9	48.8
	0.50	380	885	817	0.008	0	4.5	42.1
Slite Std <sup>g</sup>	0.30	540	767.7	938.3	0	3.6	2.5	66.9
	0.50	390	915.2	844.8	0	0	1.2	47.4
	0.40	420	880.3	845.7	0.027	1.7	4.9	60.7
Fin Rpd <sup>h</sup> + 44%SL <sup>i</sup>	0.50	390	874.1	806.9	0.01	0	4.4	46
	0.30	520	799.9	939.1	0	3.8	2.3	85.7
	0.50	410	892.3	823.7	0	0	1.4	59.9
Fin Rpd	0.40	420	858	858	0.027	1.15	4.5	55
	0.50	370	891.8	823.2	0.01	0	4.7	41.5
	0.30	540	761.9	931.2	0.01	3.8	1.6	82
Anl + 10%SF	0.40	420	863	863	0.027	2	4.7	57.6
	0.50	380	885	817	0.013	0	4.9	43.4
	0.30	540	767.7	938.3	0	4.15	2.4	66.5
P Kalk C <sup>j</sup>	0.40	420	851.5	851.5	0.08	1.42	4.8	81.4
	0.30	500	796.5	973.5	0	2.1	0.5	126.9
	0.35	450	844.1	951.9	0	1.7	0.9	112.7
P Kalk C <sup>j</sup>	0.40	420	880.3	845.7	0.03	1.7	4.8	68.9
	0.50	390	874.1	806.9	0.014	0	4.7	51.8
	0.30	530	781.2	954.8	0	3.6	2.2	98.5
	0.35	470	851	922	0	2.62	1.8	86.3
	0.50	400	903.8	834.2	0	0	1.2	60.9

<sup>a</sup> AEA – Air entraining agent, supplied by Cementa L17, percentage by mass of binder.

<sup>b</sup> Sp – Super-plasticizer, purchased from Cementa Melcrete, percentage by mass of binder.

<sup>c</sup> Compressive strength tested according to SS 13 72 10.

<sup>d</sup> Anl – Swedish structural cement (Anl ggningscement, CEM I 42,5 N - SR 3 MH/LA).

<sup>e</sup> SF – Silica fume (Elkem Microsilica, Norway).

<sup>f</sup> Fin Std – Finnish standard Portland cement blended with 15–18 % slag (CEM II/A-S).

<sup>g</sup> Slite Std – Ordinary Portland cement in Sweden, made in Slite (CEM I 52.5 N).

<sup>h</sup> Fin Rpd – Finnish rapid Portland cement blended with 10–15 % limestone filler (CEM II/A-LL 42.5R).

<sup>i</sup> SL – Finnish ground granulated blast-furnace (ggbf) slag.

<sup>j</sup> P Kalk C – Swedish Portland cement blended with 10–15 % limestone filler (CEM II/A-LL).

the laboratory, including one plain concrete specimen with a size of  $400 \times 300 \times 300$  mm and the other reinforced concrete beams with a size of  $1200 \times 300 \times 300$  mm. The plain concretes were used for the test of chloride profiles. The reinforced concrete beams were designed for the investigation of corrosion resistance of rebars in concretes under pre-cracked and uncracked conditions. Ribbed rebars with diameter of 12 mm were bended at the ends for placing them at the specific position. The end of rebars were coated with epoxy, and the length of the exposed part of rebars was about 480 mm (see Fig. 1). There are mainly two different setups of the rebars with a cover thickness of 15 mm and 30 mm, respectively. Some rebars were also embedded in concrete with a cover thickness of 60 mm above the set of bars with a cover thickness of 30 mm. A copper wire was soldered on one of the ends of rebar. The other end of the copper wire was connected to a plinth in a nearby electronic box for electrochemical measurement. The detailed information of the setting of reinforcements in concretes can be found in the report [23] and there is a manual for how the rebars were cast in each specimen [24].

## 2.2. Field exposure conditions

The field exposure site has been established in the autumn of 1996 at the highway 40, which locates outside Borås in Sweden. As shown in Fig. 2, specimens were mounted in steel frames at the road level and then were put upon the gravel layer. To ensure the traffic safety, the exposure site was separated from the road by a guard rail. A part of the guard rail kept open (below the height of 0.45 m) to ensure the specimens fully exposed to the splashing water from the traffic. The distance between the exposure surface and safe line of road is about 2.7 m. The specimens were exposed to many winters with low temperature, moist environment, and de-icing salts. This kind of climate corresponds to the exposure class equal to XD3/XF4 according to EN 206-1. Fig. 2 also shows the sampling position for the measurement of chloride profiles. The air temperature at a weather station close to the exposure site was about  $10^\circ\text{C}$  as a monthly average. The detailed condition of the exposure site can be found in the report [13].

## 3. Experimental methods for testing chloride penetration profiles and rebar corrosion

### 3.1. Measurement of chloride penetration profiles

After an exposure of about 1, 5, 10 and 20 winters, the concrete blocks were taken to the laboratory for sampling. Concrete cores with diameter of 100 mm, from the middle height of the vertical exposure surface, were collected for the measurement of chloride profiles (see Fig. 2). The samples were taken at a certain depth by a diamond tool on a

lathe step by step from the surface of exposure. The sampling depth was measured with an accuracy of 0.5 mm by a caliper. The samples were dried at  $105^\circ\text{C}$  immediately after the grinding. Afterwards the dried samples were stored in a desiccator until the analysis for chloride content.

The total chloride content in each sample was analyzed by means of potentiometric titration principally based on AASHTO T260 with acid extraction.

### 3.2. Measurement of reinforcement corrosion

After exposed for 10 and 20 winters, the corrosion level of the rebars in the reinforced concrete beams were estimated by the use of one handheld instrument RapiCor, which is based on the galvanostatic pulse technique, as described in [13,25,26]. This instrument measures three parameters: the corrosion rate; the half-cell potential of a rebar inside the concrete and the ohmic resistivity of the concrete cover. These parameters were utilized for the assessment of the corrosion condition. The main parameter from this instrument is corrosion rate, integrating with the resistivity and half-cell potential as the complementary parameters for assessing the level of corrosion or corrosion index. Table 2 shows the criteria of corrosion index used in this study. The green, yellow, orange and red color present the corrosion of steel bar with a level of negligible, low, moderate and high, respectively.

After a nondestructive measurement of corrosion on the concrete surfaces, some of the beams containing suspiciously corroded rebars were selected for destructively examination of corrosion condition. These beams were firstly sawn at the position where one end of rebar laid in the transvers section to the cross-section of the exposed rebar. Then the RapiCor instrument was used again to measure the corrosion with the sure connection to the rebar (to check if there was any misleading result from the measurement by connection of the soldered cable). The rebars were collected by means of sawing and splitting from each concrete beam. The actual condition of corrosion in each rebar was examined by a visual observation as well.

### 3.3. Measurement of carbonation depths

For some selected types of concrete, the carbonation depths on the split surfaces were measured by using the colorimetric method with 1 % phenolphthalein solution. It should be noted that no systematic measurement of carbonation depths was planned in the research program, but just occasionally carried out on some types of concrete for destructive tests, such as those after removal of rebars or on the small specimens for testing frost attack.

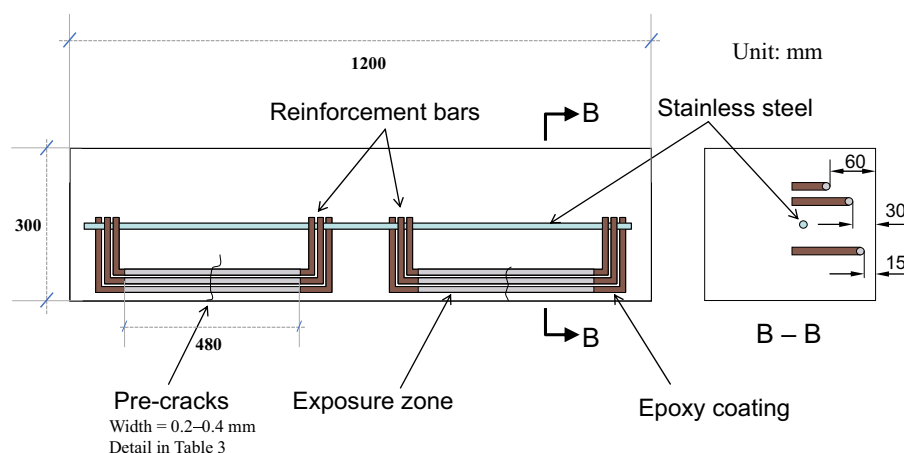


**Fig. 1.** Arrangement of rebars in the reinforced beams exposed to the Rv40 field site [17].

Notes: 1) There was no rebar located at the level with a cover thickness of 60 mm in most of the beams. 2) Each rebar was soldered with a copper wire which connected the rebar to the plinth in a box outside the specimen for the measurement of corrosion by the electrochemical method.

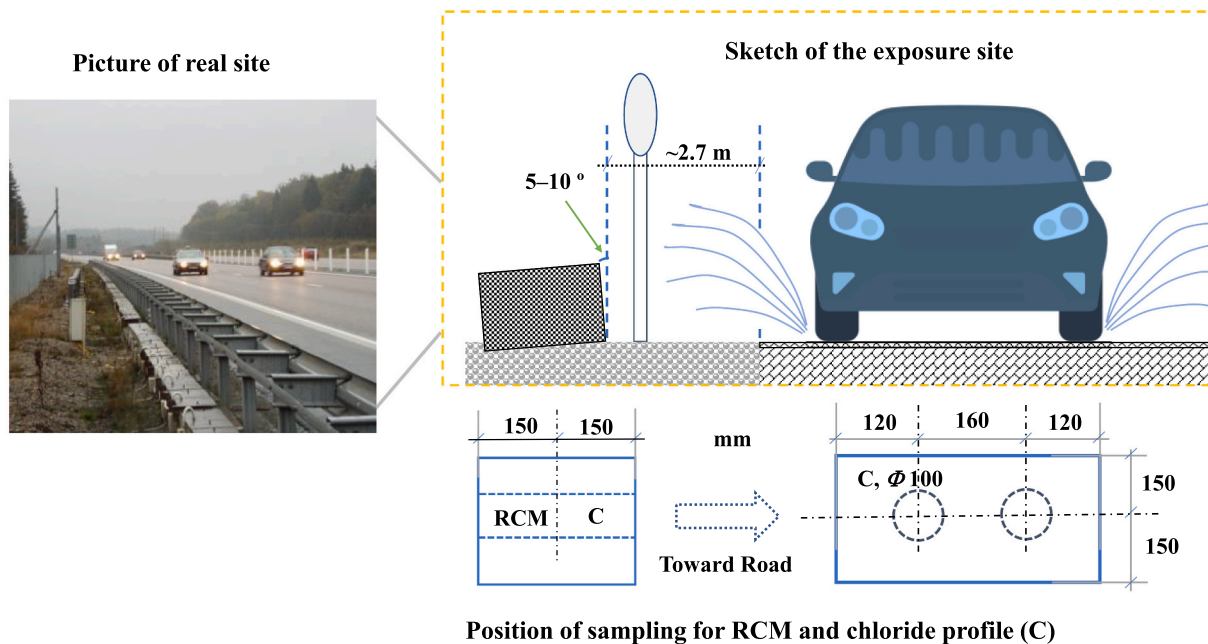


Fig. 2. Placement of specimens at the Rv40 field site for exposure.

Table 2  
Criteria for different indexes of reinforcement corrosion.

Corrosion Index	Corrosion level	Corrosion rate $\mu\text{A}/\text{cm}^2$	Resistivity $\Omega\cdot\text{m}$	Half-cell potential $\text{mV}_{(\text{CSE})}$
1	Negligible	<0.1	-	-
		0.1~0.5	> 10	> -200
2	Low	0.1~0.5	< 10	< -200
		0.5~1	> 10	> -200
3	Moderate	0.5~1	< 10	< -200
		>1	> 10	> -200
4	High	>1	< 10	< -200

#### 4. Performance of concrete and reinforcement

##### 4.1. Resistance to chloride penetration

###### 4.1.1. Effect of binder types

Fig. 3 presents the comparison of chloride penetration profiles in concrete with five different types of commercial cements after exposed for 20 winters. It is difficult to find a general tendency in the chloride content at the specific depth with different types of cements, so there is no absolute ranking of the resistance to chloride penetration for different commercial cements with different  $w/b$ . For the concretes with  $w/b \leq 0.4$ , the Fin Rpd cement has the lowest chloride contents in most of the depths. An increase in  $w/b$  generally induces a deeper chloride penetration into the concretes.

The effect of mineral additions (silica fume and slag) on the chloride penetration is shown in Fig. 4. It seems that a replacement of Swedish structural cement by 5% silica fume has no significant effect on chloride penetration after 20 years exposure, but its effect on reducing chloride content becomes clear when it is replaced with 10% silica fume. For concretes with  $w/b = 0.3$ , the blending of 44% slag has minor effects on chloride penetration. This is mainly because of the limited hydration degree of slag and clinker. According to Powers's model [27], a full hydration of typical Portland cement requires at least a  $w/b$  of 0.36, so

slag in concretes with  $w/b$  of 0.3 has a low accessibility to water at later age to limit its refinement effect on the pore structure. Yio et al. [28] reported that the slag blended pastes with  $w/b$  of 0.3 had a higher gas transport coefficient than the plain paste. A recent study also found that slag had a much weaker effect on chloride migration coefficient of pastes with  $w/b$  of 0.35 than those with  $w/b$  of 0.45 at 6 months [29]. Therefore, when the concretes are mixed with  $w/b$  of 0.4–0.5, the reducing effect from slag is much clearer especially in the depth larger than 20 mm. This mainly derives from the effect of slag on refining the pore structure, such as reducing the pore connectivity [30], and changing the chloride binding capacity [31,32].

###### 4.1.2. Effect of $w/b$ and the entrained air

Fig. 5 presents the chloride penetration profiles in concretes mixed with different  $w/b$ , and with/without entrained air after an exposure of 20 winters. It is evident that a decrease in  $w/b$  enforces concretes with a higher resistance to chloride penetration. This phenomenon is more obvious in concretes with  $w/b$  larger than or equal to 0.40, but there is one exception in the concrete with the binder noted as Fin Rpd + 44%SL. In this mix the chloride penetration profile is quite similar in concretes with  $w/b$  of 0.40 and 0.50.

The effect of AEA on chloride penetration in the concretes with  $w/b$  of 0.5 is shown in Fig. 6. For the concretes mixed with Anl and Anl + 5%

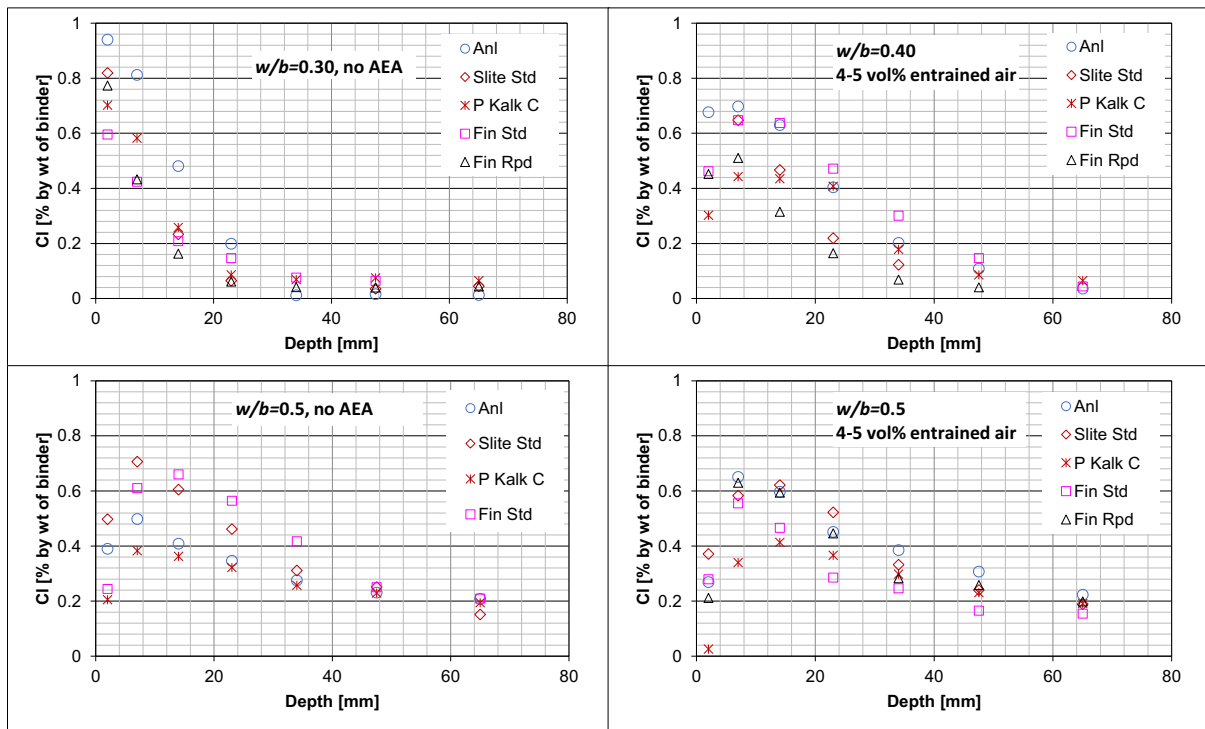


Fig. 3. Comparison of chloride penetration profiles in concretes cast with different types of commercial cements.

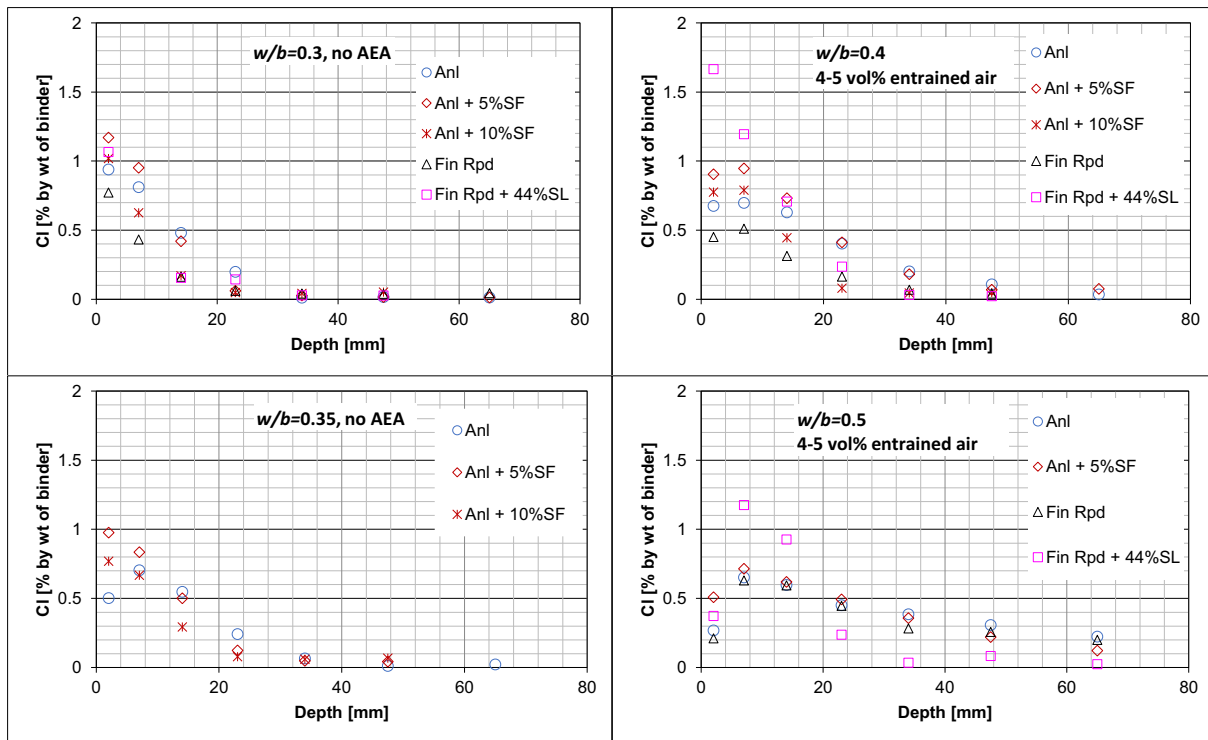


Fig. 4. Comparison of chloride penetration profiles in concretes with the addition of different supplementary cementitious materials.

SF (see Fig. 6, left side), the introduction of entrained air void induces a higher chloride content from the surface and to the depth at about 60 mm. In the deeper place up to 120 mm, the chloride content in concretes with AEA stays close to that in concrete without entrained air. However, the entrained void seems to have little influence on the resistance to chloride penetration in concrete mixed with Slite Std or P Kalk C cement

(see the right side in Fig. 6). Therefore, it is obvious that the effect of AEA on chloride penetration in cement-based materials depends on the types of binders.

#### 4.1.3. The influence of different exposure durations

The chloride penetrations in two mixes of concrete with  $w/b$  of 0.4



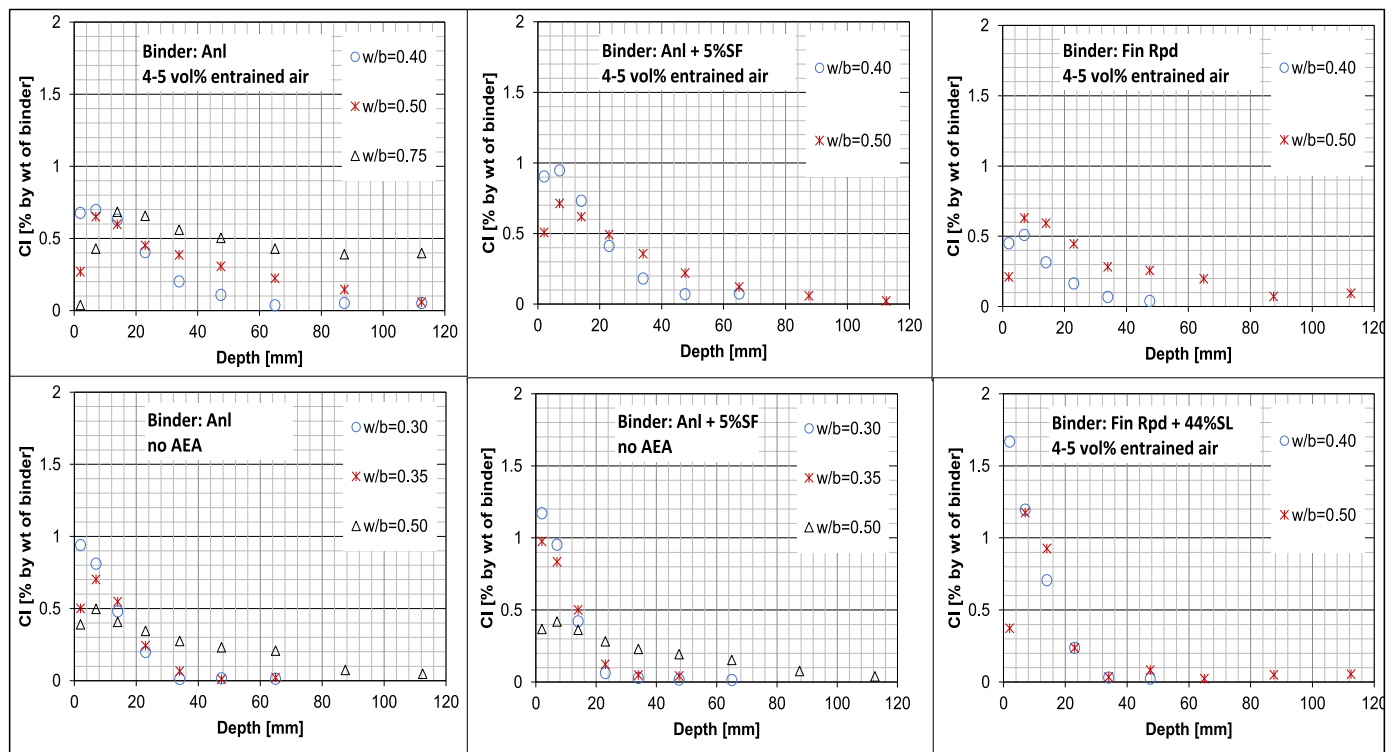


Fig. 5. Chloride profiles in concretes with different w/b, binder types and AEA contents.

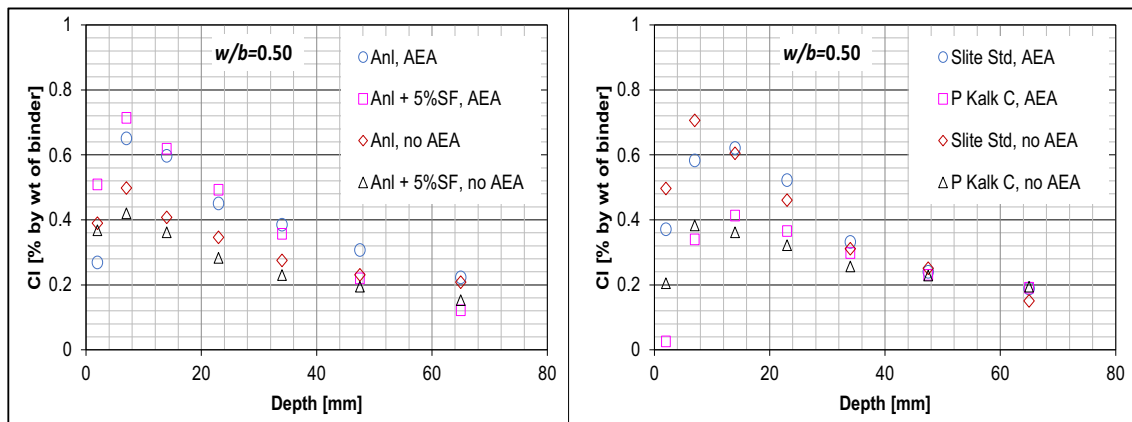


Fig. 6. Chloride profiles in concretes with and without AEA after 20 winters exposure.

are compared in Fig. 7 to focus on the effect of different exposure durations. The chloride profiles in concretes with Swedish structural cement (Anl) are similar in different exposure durations from 1 to 10 winters, and the value is evidently lower than that of concretes after an exposure of 20 winters. An interesting phenomenon has been observed in concrete with Swedish structural cement replaced with 5 % SF. The chloride content in the depth of 0–20 mm was unexpectedly higher in concretes with a shorter exposure duration. After four winters from 1996 to 2000, a new technique was used for spreading the de-icing salts and the average dosage was reduced to a half of the previous winters [13], so this may result in a lower free chloride concentration in pore solution. However, the free chloride in pore solution accounts for <10 % of total chloride content, and the main contribution is from bound/absorbed chloride in solid phase (AFm and C-S-H) [33]. Therefore, this interesting difference may result from phases change after a long-term interaction and leaching, such as decomposition of chloride-containing AFm, leaching of portlandite and decalcification in C-S-H [33,34]. Moreover,

the carbonation in the near surface zone is also one of the main factors. Carbonation will induce a decrease in the pH of pore solution, this process may increase the Cl binding when the pH lowers from 13 to 12 and the binding capacity would decrease when the pH decreases after 12 [35]. Hence, the surface zone could have a higher chloride content at 5 years than later age due to the limited carbonation.

Fig. 8 shows the comparison of chloride penetrations in all concretes with  $w/b \leq 0.4$  after exposure of 10 and 20 winters. The chloride penetration depths in concretes after an exposure of 20 winters are generally deeper than those in concretes after an exposure of 10 winters. However, the minor differences in concretes with  $w/b$  of 0.3 indicate that for these types of concretes the penetration under the road environment is rather slow after the 10-winter exposure.

#### 4.1.4. Effect of the exposure environment

The chloride profiles in concretes with Anl cement exposed to marine environment have been reported in a previous study [16] after a 20-

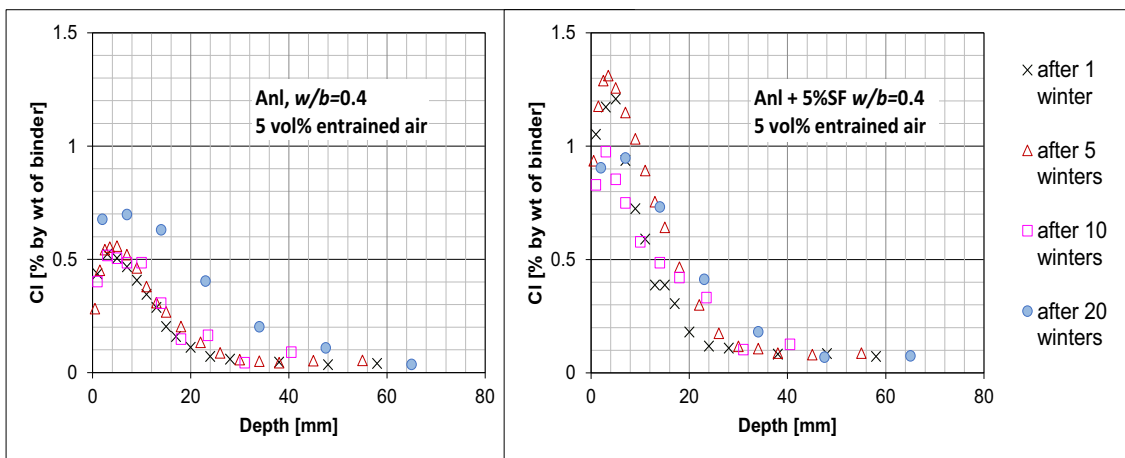


Fig. 7. Chloride profiles in two selected types of concretes after the exposure of different durations.

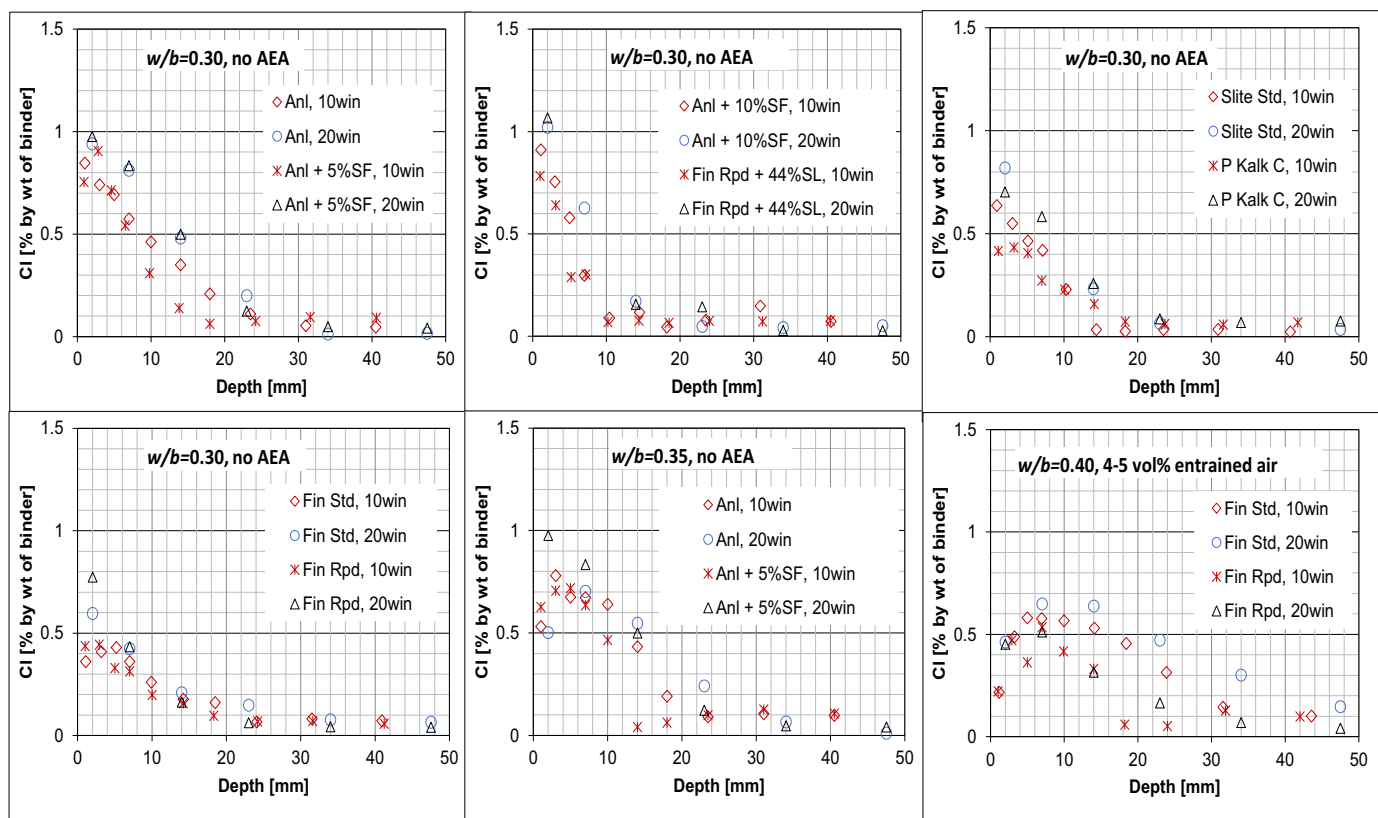


Fig. 8. Chloride profiles in different concretes after an exposure of 10 and 20 winters (win = winter).

year-exposure along Swedish western coast. Fig. 9 presents the comparisons of chloride penetration profiles in four similar concretes exposed to different environments (marine atmospheric, marine splash and de-icing salt road). Apparently, an exposure in the marine environment, especially in splash zone, induced a higher chloride content than that in the road environment in all depths. After an exposure of 20 winters/years, the chloride penetration in concrete with Swedish structural cement (Anl) and  $w/b$  of 0.35 is severer in marine atmospheric environment than that in road environment. For the concretes with 5 % SF, the difference in chloride profiles between marine atmospheric and road environment is less than that of concretes with plain Swedish structural cement. However, it is worth to note that the concretes with  $w/b$  of 0.35 at the highway site were not mixed with any AEA but this

was used in the mixes exposed at the marine site. The chloride ingress process is moisture dependent as well. A higher moisture content induces a larger chloride migration [36], so the marine environment induces a severer ingress of Cl than road environment. Leaching would cause the coarsening of microstructure to induce a peaking phenomenon in concretes at marine exposure [34,37]. Moreover, splashing zone has a much higher frequencies wet-dry cycles to induce severer leaching and precipitation on the surface zone. This results in a more evident phase change of products and microstructure changes compared to atmospheric zone and road environment, so we can observe a much higher ingress and peak of chloride content.



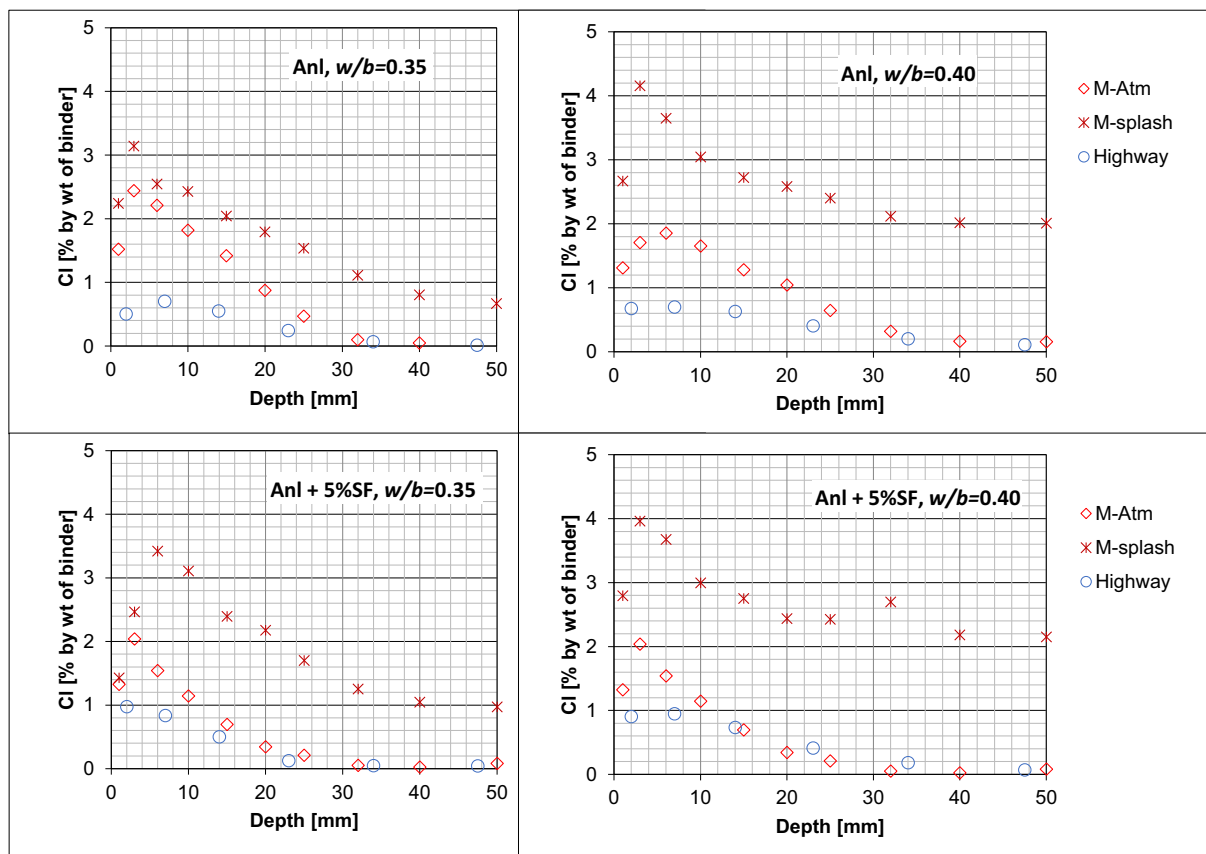


Fig. 9. Chloride penetration profiles in concretes after an exposure of 20 winters/years under the M-Atm (marine atmospheric), M-splash (marine splash) and highway (de-icing road) environments.

#### 4.2. Resistance to reinforcement corrosion

It has been proven through several destructive examinations that the measured corrosion index by the handheld instrument RapiCor were in reasonable agreement with the visual observation [25,38,39]. Because the rebars with 15 mm cover thickness in the lower part of the beam that was covered by the snow for a longer period than the rebars with 30 mm cover, these rebars revealed less corrosion than those with 30 mm cover. The chloride penetration profiles were sampled at the same level as the rebars with 30 mm cover. Therefore, we summarize the measured corrosion indexes for the rebars with 30 mm cover only (see Table 3). Fig. 10 shows a typical comparison between the visual examination and the RapiCor measured corrosion state of reinforcement.

Table 3 shows that a low corrosion (index 2) occurred in five types of uncracked concrete with  $w/b$  of 0.40–0.50 after 20 winters. Moderate to high corrosion (indexes 3–4) occurred only in four different uncracked concretes with  $w/b$  larger than or equal to 0.50. The blending of slag and silica fume can significantly inhibit the corrosion of rebar in concrete with the same  $w/b$ . It was expected that corrosion occurred more in types of pre-cracked concrete. From two occasional measurements of corrosion, it is difficult to know the actual initiation of corrosion. However, if we take corrosion index 2 (low corrosion) as the near initiation, we can roughly estimate a critical chloride content for the initiation of corrosion at the depth with about 0.3 % by mass of binder for most of rebars in uncracked concrete. For the rebar in concrete with Fid Rpd cement and  $w/b$  of 0.5, a moderate corrosion occurred even at the depth with chloride content of 0.1 % of binder by mass. This rebar was released for visual examination and rust stains were indeed observed [13]. No good explanation can be given for this observation from current investigations. It seems that the critical chloride content of corrosion of rebars is lower in the pre-cracked concrete cover than that

in the uncracked. However, a further investigation is needed for drawing a clear conclusion.

#### 4.3. Resistance to carbonation

As mentioned in Section 3.3, the carbonation depths were measured only in some selected types of concrete. The measured results are listed in Table 3 in the column after the corrosion index of rebars in the uncracked concrete. It is obvious that the carbonation only occurs in a thin layer close to surface. For the concretes with  $w/b \leq 0.5$ , the carbonation depth is <3 mm after 20 winters. Even for concretes with  $w/b$  of 0.75, the carbonation depth is only 3–6 mm after 10 winters. From data in a parallel project for frost attack, the concrete with CEM III/B (slag content 66–80 %) and  $w/b$  0.5, the carbonation depth was 5–6 mm after 20 winters [40]. Therefore, it can be concluded that all the types of concrete in this study should have a good resistance to carbonation under the de-icing salt road environment.

The composition at the surface after 20-year was altered due to carbonation [41]. Some investigations ascribe the peak phenomenon to the carbonation induced phase and microstructure change [35,37]. Carbonation is one the factor for peak of chloride content, but it can be observed that the influential depth of carbonation is much lower than the peak position. Therefore, leaching of hydration products and interaction between de-icing salts and concrete make large contributions in the formation of peaks as well.

### 5. Modelling of the chloride penetration

According to the previous publications [13,15], the ClinConc model performed a better prediction of the chloride penetration in concretes exposed to the de-icing environment among three different kinds of

**Table 3**  
Corrosion indexes of steel bars with 30 mm cover in concrete beams after an exposure for 20 winters.

Binder	Uncracked					Pre-cracked	
	w/b	air vol %	Cl%-binder at the rebar	Corrosion Index	Carbonation depth [mm]	Crack [mm]	Corrosion Index
Anl	0.40	4.8	0.3	2	1-2	0.2	2
	0.50	4.5	0.3	2	1-2	0.2	1
	0.30	1.3	0.1	1		0.2	2
	0.35	0.9	0.1	1		0.3	1
	0.50	1.3	0.3	3		0.3	3
	0.75	4.5	0.9	4	3-6	0.2	4
Anl + 5% SF	0.40	4.7	0.3	1		0.2	1
	0.50	4.4	0.15	1		0.4	1
	0.30	1.2	0.1	1		0.2	1
	0.35	1.1	0.1	1	1-2	0.4	1
	0.50	0.9	0.3	1	2-3	0.3	2
Fin Std	0.40	4.9	0.15	1	0-1	0.4	1
	0.50	4.5	0.3	1		0.3	2
	0.30	2.5	0.1	1		0.3	1
	0.50	1.2	0.5	4		0.4	3
Slite Std	0.40	4.9	0.1	1		0.2	2
	0.50	4.4	0.4	1		0.4	1
	0.30	2.3	0.1	1		0.4	1
	0.50	1.4	0.4	2		0.4	2
Fin Rpd + 44%SL	0.40	4.5	0.1	1		0.4	1
	0.50	4.7	0.2	1		0.3	1
	0.30	1.6	0.1	1		0.4	1
Fin Rpd	0.40	4.7	0.1	1		0.4	2
	0.50	4.9	0.1	3	0-1	0.4	3
	0.30	2.4	0.1	1		0.3	1
Anl + 10%SF	0.40	4.8	0.1	1		0.4	1
	0.30	0.5	0.1	1		0.2	1
	0.35	0.9	0.1	1		0.2	2
P Kalk C	0.40	4.8	0.1	2		0.2	2
	0.50	4.7	0.1	1		0.4	1
	0.30	2.2	0.1	1		0.2	3
	0.35	1.8	0.1	1		0.2	1
	0.50	1.2	0.3	2		0.3	3

Note: Italic values were measured after exposed for 10 winters.

models including the simplest model based on Fick's law, the probabilistic model DuraCrete and the mechanism-based model ClinConc. Kim et al. [42] reported that it also worked well in the prediction of chloride profiles in concretes under different marine exposure environments. Therefore, the ClinConc model will be used as the basic model for a further modification. A more detailed information of this model has been described in [7].

5.1. The main input data

The main input parameter in ClinConc model is the chloride migration coefficient of concrete at the age of 6 months, measured by the RCM test according to the Nordtest standard NT BUILD 492. Because the RCM test was not standardized in 1997, the coefficients were not tested

at the ages of 6 months. Therefore, the migration coefficient by RCM from some previous studies were adopted to obtain some empirical equations by regressions. Fig. 11 show that the relationship between chloride migration coefficient and w/b follows a power function.

$$D_{RCM} = A \left(\frac{w}{b}\right)^B \tag{1}$$

where constants A and B depend on binder type and dosage of AEA. The regression equations in Fig. 11 were used for estimating the chloride migration coefficient in the relevant types of concrete.

5.2. Other input data

When the de-icing salt is splashed on the concrete surface, the

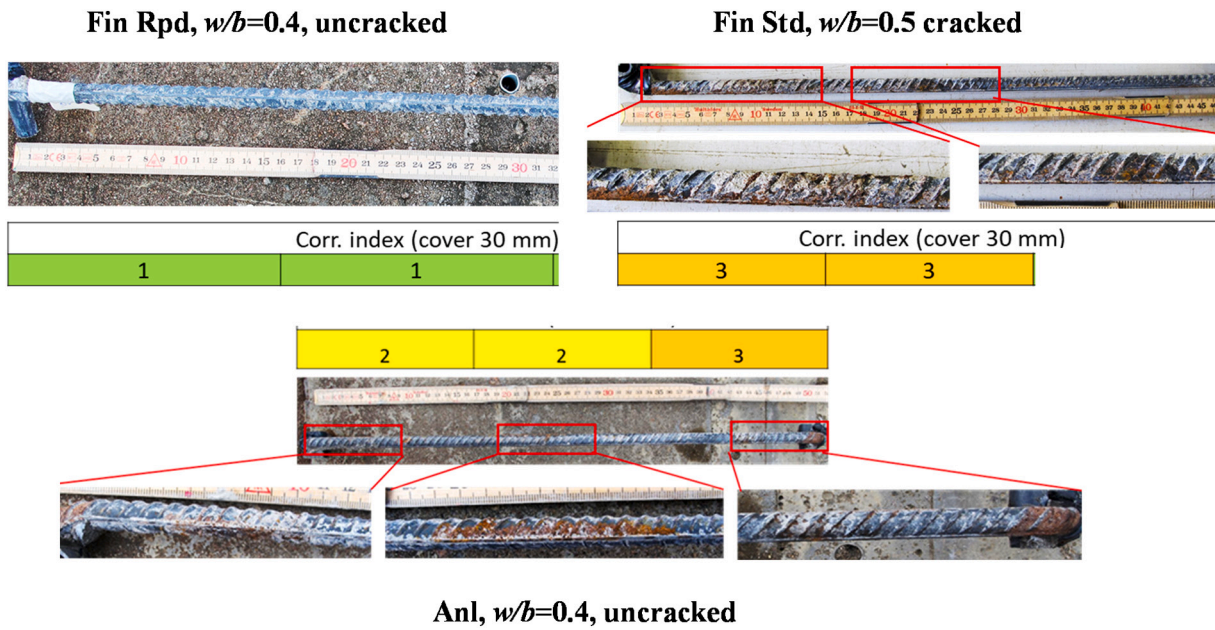


Fig. 10. Comparison between RapiCor measured corrosion and visual examination.

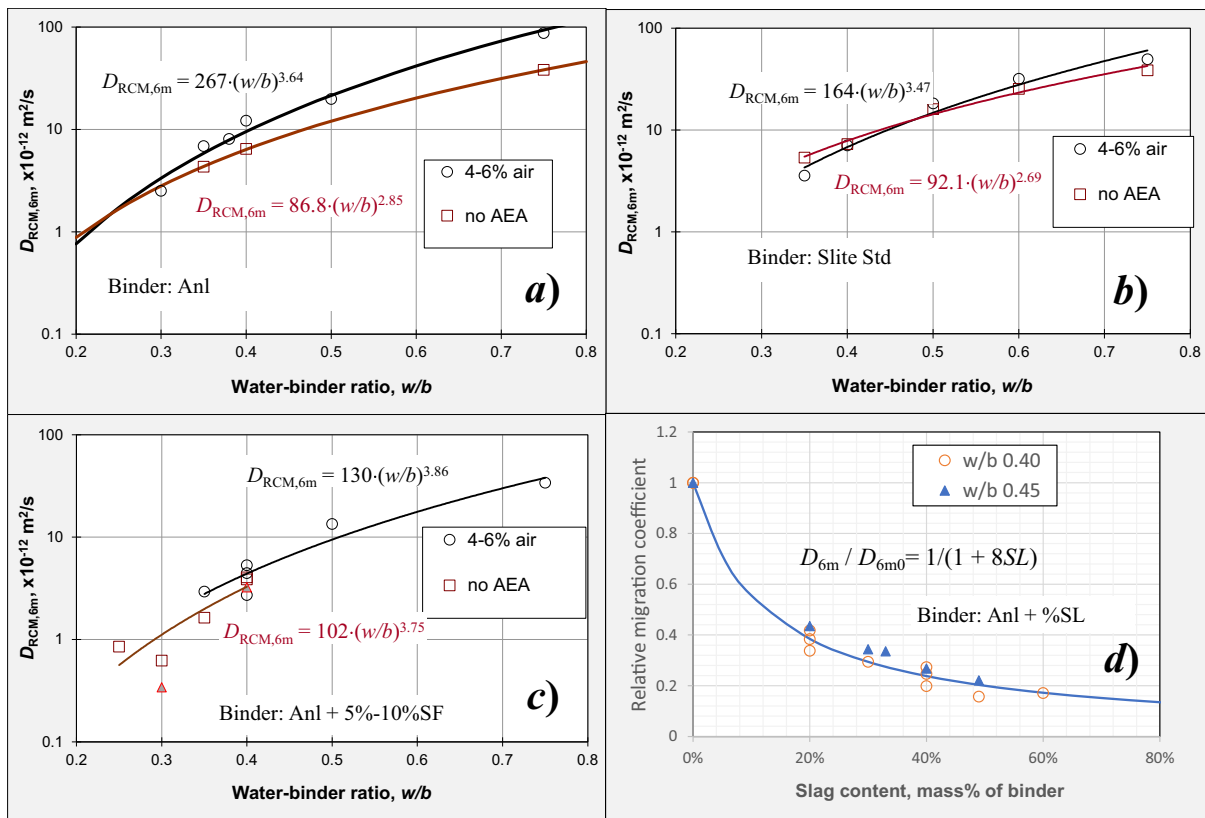


Fig. 11. Relationship between  $D_{RCM}$  and  $w/b$  or  $D_{RCM}$  and slag content: in a) to c) the data were adopted from [43], and the data in d) were adopted from [44].

chloride penetration occurs during the whole year, even though the surface concentration may dramatically change from saturated concentration (as unmelt de-icing salt) to zero (after heavy raining or road washing). It is difficult to know the actual variation of chloride concentration on the surface of concrete. Therefore, the environmental data were adopted with the chloride concentration of 1.5 g/l and the mean annual temperature of 10 °C which has been used in our previous

simulation for concretes under road environment [13,15]. The initial chloride concentration in each concrete has been estimated by the evaporable water content with the chloride content of 15 mg/l in mixing water. The initial alkali content in cement and slag was calculated by the data from manufacturers. The age factor for chloride binding has been taken as 1/3 of the value under submerged environment. The expansion factor and the age factor due to drying were not taken into

consideration. Some other parameters in the model use the same value as those described in [10] or [15]. More detail of input parameters can be found in Table A1.

### 5.3. Simulation by the previous ClinConc model

By adopting the input data presented in 5.1 and 5.2 into ClinConc model, we get the modelled data in Fig. 12 to compare with the measured profiles. The modelled penetration depths seem to fairly agree with the measured chloride ingress. However, there are large differences between the predicted profiles and the measured data, especially in concretes with high  $w/b$  ( $\geq 0.4$ ). A peak occurs near surface zone in most of the chloride penetrations in concretes with  $w/b$  larger than or equal to 0.35, and this results from the drying-wetting cycles [45], carbonation and interaction of de-icing salts on concrete surface exposed to the road environment. Therefore, it is difficult to make an accurate prediction on the total chloride content by models based on the Fick's law.

A further modification is needed for the previous ClinConc model so that the modelled profiles become closer to the measured value. The fair match between the modelled chloride penetration front and the measured one implies that the predicted free chloride content in the deeper part of concrete is reasonably correct. Thus, the abnormal shape of chloride penetration profiles may be because of the change in the binding behavior in the lower depth of penetration. The distance from surface to the peak point is designated as  $x_{peak}$  in our modification. The value of  $x_{peak}$  were collected from the measured chloride content and presented in Fig. 13. The correlations between  $x_{peak}$  and  $w/b$  can be expressed by a logarithmic function as shown in the formulation of Eq. (2). The values of parameter,  $\alpha$  and  $\beta$ , of different binders are shown in Table 4.

$$x_{peak} = \alpha_p \ln\left(\frac{w}{b}\right) + \beta_p \quad (2)$$

### 5.4. Further modification of ClinConc model

The peak phenomenon of chloride profile in concretes was often attributed to effect of drying-wetting cycles on pore solution in some literatures [45–47]. However, we strongly believe that both carbonation and calcium redistribution or leaching play a critical role in the chloride binding behavior of pastes. It has been proven that, after carbonation, the chloride binding capacity dramatically decreased due to the changes in the pore structure [48,49], pore solution [19,50], phase assemblage [50–52] and moisture condition [49,53]. However, as shown in Section 4.3, the carbonation depth for most of types of concrete in this study is  $< 3$  mm, which is markedly less than the peak depth. Therefore, the lower chloride content in the near surface zone may only partially be attributed to the effect carbonation on the surface. The Monte Carlo simulation was performed in this study to reveal the dissolving behavior of portlandite ( $\text{Ca}(\text{OH})_2$ ) in solutions with various chloride concentrations. The saturation index ( $SI$ ) of portlandite is calculated according to the formula.

$$SI = \log\left(\frac{Q}{K}\right) \quad (3)$$

where  $Q$  is the ion activity product, and  $K$  is the equilibrium constant of ion product. The dissolution of portlandite has been predicted by a simple calculation based on the saturation index. Fig. 14 shows that the  $SI$  of portlandite will decrease as the increase in concentration of NaCl. Therefore, as the chloride content increases during its penetration into concrete, more portlandite will dissolve into solution due to the decrease in the saturation degree of pore solution. Moreover, calcium ions in the near surface zone will be washed by the rain or splashed water, so it induces the inner Ca ions move to the surface. This process will cause the change of the pore structure and the chloride binding capacity of pastes in the near surface zone. However, the combining effect of carbonation and leaching is difficult to be quantified by theoretical model or

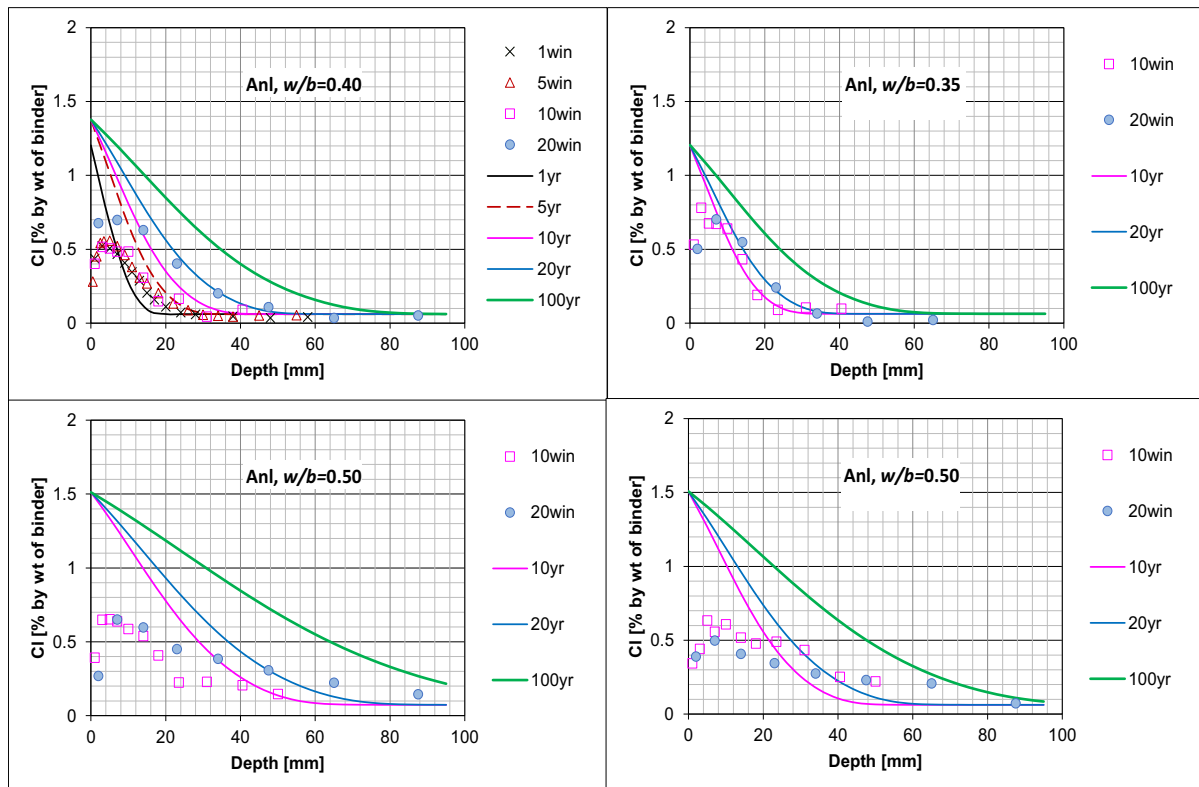


Fig. 12. Comparison of some of the measured (marks, win = winter) and predicted (lines, yr = year) chloride profiles in concrete by the previous ClinConc model.

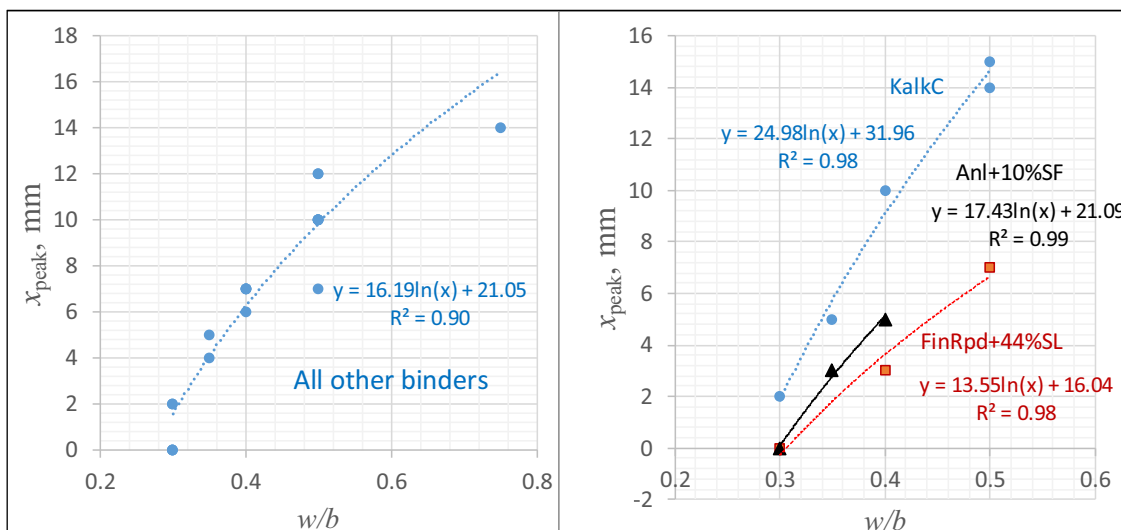


Fig. 13. Correlations between  $x_{peak}$  and  $w/b$  in concretes with different binders.

Table 4

Parameters for the calculation of peak position in Eq. (2).

Binder	$\alpha_p$	$\beta_p$
Anl, Slite Std, Anl + 5%SF, Fin Std, Fin Rpt	16.2	21
Fin Rpt + 44%SL	13.6	16
Anl + 10%SF	17.4	21
P Kalk C	25.0	32

experimental method. Hence, two empirical equations (see Eq. (4)) are proposed to describe the redistribution of bound chloride content in the near surface zone of concretes exposed to the road environment.

$$f_{red} = \begin{cases} \left[ 1 - k_1 \cdot c_f \cdot \frac{(x_{peak} - x)}{x_{peak}} \cdot \sqrt{\frac{w}{b} - b_0} \right] \cdot k_2 \cdot \sqrt{\frac{w}{b} - b_0} & x \leq x_{peak} \\ k_2 \cdot \sqrt{\frac{w}{b} - b_0} & x > x_{peak} \end{cases} \quad (4)$$

where  $f_{red}$  is the redistribution factor of the bound chloride applied in ClinConc model, and  $c_f$  is the concentration of free chloride predicted using the ClinConc model. The parameters  $b_0$ ,  $k_1$  and  $k_2$  are constants and their values for different binders are shown in Table 5.

A “trial-and-error” approach was applied to obtain constant values in Eq. (4), and Table 5 presents parameters for different binder systems. Some interesting information can be observed about the long-term behavior of binders. The  $k_1$  constant indicates the degree of reduction in the chloride binding capacity on the surface zone. This value of binders containing slag or limestone is higher than that of other binders, which indicates a larger reduction in the chloride binding, and this may be because of a weaker resistance to leaching and a larger change in compositions due to leaching, carbonation, and interaction of de-icing salts with hydration products. The constant  $k_2$  means the general extent of decrease in the chloride binding capacity near the concrete surface zone. The binder with limestone (P Kalk C) has the lowest value, and this may be due to the weak interaction between limestone and chloride ions. The constant  $b_0$  indicates a critical  $w/b$  with which value

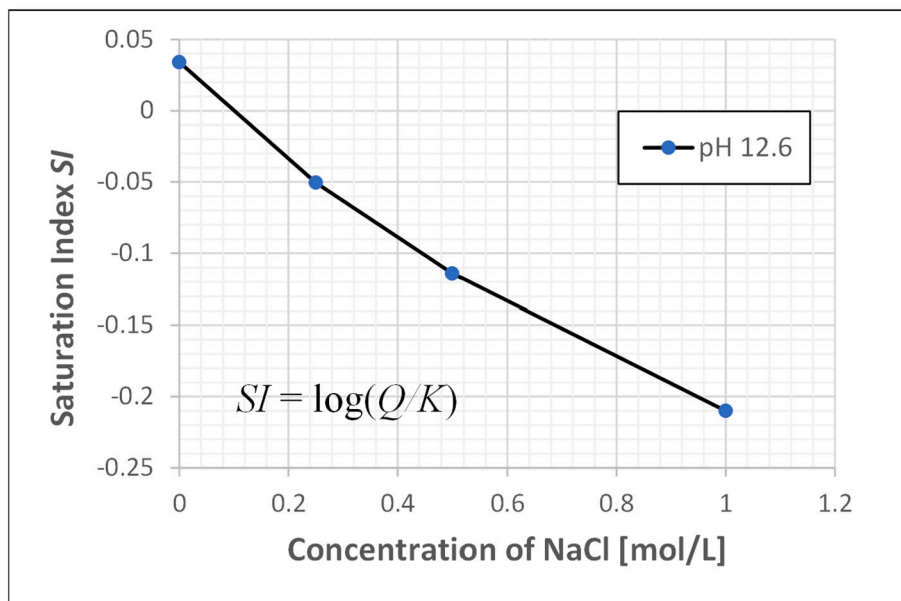


Fig. 14. Saturation index of portlandite in solution with different concentration of sodium chloride.



**Table 5**

Value of constants applied in the calculation of chloride redistribution factor in Eq. (4).

Binder types	$b_0$	$k_1$	$k_2$
Anl, Fin Rpt, Slite Std	0.3	1	1
Anl + 5 %–10%SF	0.35	1	1
Fin Std	0.3	1.5	1
Fin Rpt + 44%SL	0.4	2	1
P Kalk C	0.3	2	0.75

the surface of concrete has no significant decrease in the binding capacity of chloride. The blending of SF (5 %–10 %) and slag (44 %) will bring an increase in this value, which results from the finer microstructures and a less diffusible matrix compared with other binders.

Fig. 15 illustrates more detailed difference between ClinConc and the modification. The predicted results of Swedish structural cement are shown in Fig. 16, and those for the other types of binders are shown in Figs. A1 to A4 in the Appendix. From these figures, it can be observed that the modelling of this modified ClinConc model have a good match with the measured chloride profile in majority of concretes with different binders and various  $w/b$ . Apparently, the modified ClinConc model performs reasonably well in the most cases including the description of chloride contents and front of penetration.

Consequently, it enables to perform the modified prediction of chloride penetration in concretes under the de-icing salt environment in the following way:

1. Calculate free and bound chloride content in concretes by the use of the ClinConc model as previously described in [15];
2. Calculate the redistribution factor of chloride by Eq. (4), and then recalculate the bound chloride profiles by multiplying the factors;
3. Finally, the total chloride profiles in concretes are calculated by the modified values as previously described in [15].

## 6. Concluding remarks

The long-term performance of many concrete blocks has been

investigated by means of both experiments and modelling. These concretes were exposed to the de-icing salt environment around a highway in Sweden up to 20 years. Based on the electrochemical measurement and the visual examination of the rebars in concrete beams, the corrosion condition is well assessed after exposed to a de-icing salt road environment. The following conclusions can be drawn based on the experimental and modelling results.

- The performance of five types of the commercial cements regarding resistance to chloride penetration are heavily dependent on the  $w/b$ . For  $w/b \leq 0.4$ , Finnish rapid cement (Fin Rpd) concrete presents the best resistance to chloride penetration among these cements. The blending of silica fume and slag improves the long-term performance of concretes. The replacement of cements by both 10 % silica fume and 44 % slag can reduce chloride penetration at all investigated ages.
- The threshold content of chloride in concretes with  $w/b$  0.5 is about 0.3 % of binder by mass. For concretes with  $w/b \leq 0.4$ , the penetration chloride content at depth of 30 mm is generally lower than this threshold value after an identical exposure duration. With the uncracked concrete cover, the rebars started to corrosion at the critical chloride content of approximately 0.3 % of binder mass. A lower critical chloride concentration seems to be detected for the initiation corrosion of rebars in concretes with the pre-cracked concrete cover.
- The chloride penetration in concretes exposed to the de-icing salt in a Swedish road environment is much slower than that in concretes exposed to the Swedish marine splash zone as well as atmosphere zone after 20 years.
- The results of long-term exposure in this study demonstrated again that the corrosion assessment by RapiCor instrument, a non-destructive measurement device, is in a good agreement with the findings from the visual examination.
- Generally, The ClinConc model presents a reasonably good prediction of the penetration front of chloride into bulk concrete, but it has a poor prediction on the chloride content near the surface zone. Therefore, it has been modified by taking the redistribution of bound

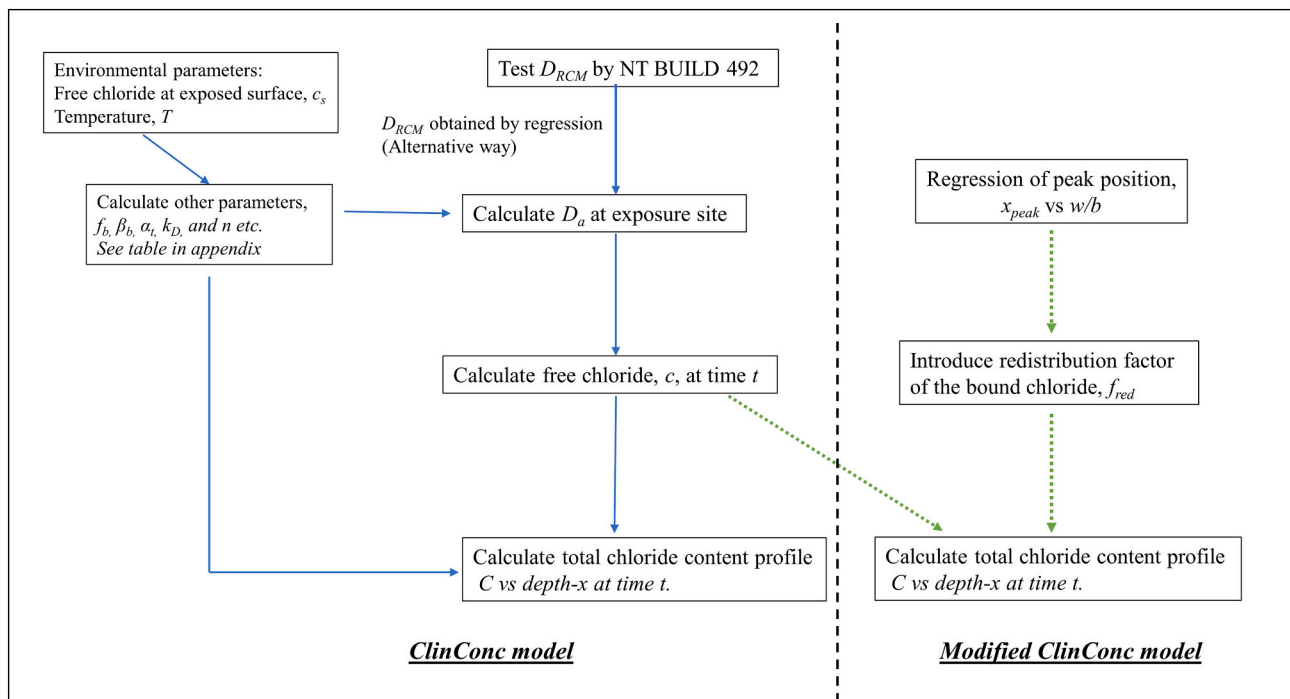


Fig. 15. Flow chart about the operation of ClinConc and the modification of it.



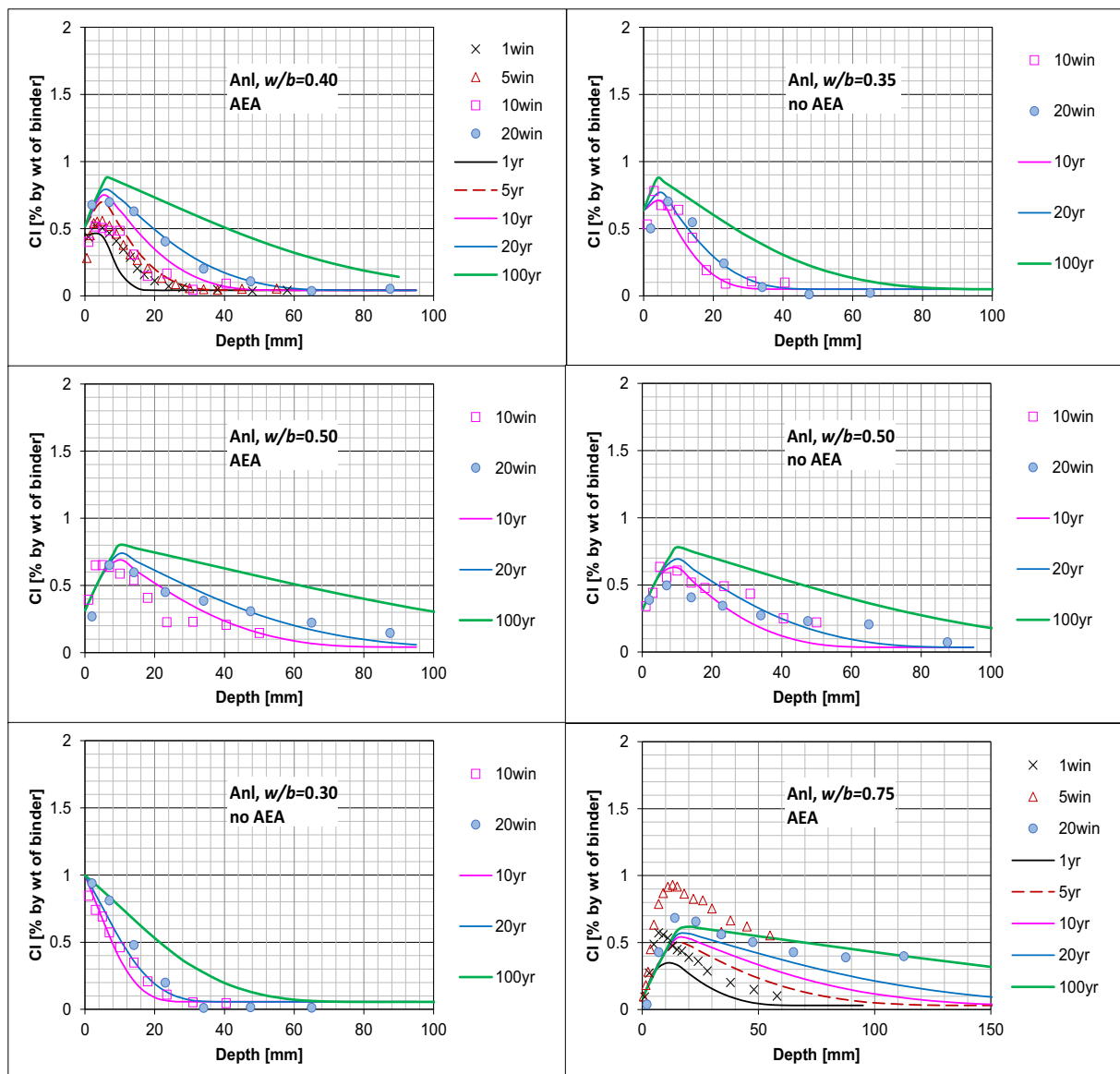


Fig. 16. Comparison of the measured (marks, win = winter) and predicted (lines, yr = year) chloride penetration profiles in concretes with Anl cement.

chloride into consideration. The modified model performs very well in the description of the chloride penetration profiles in all depth, proving by a good match between the measured and modelled chloride content.

**CRedit authorship contribution statement**

*Luping Tang:* Conceptualization, Methodology, Investigation, Data analysis, Writing-Original Draft, Revision & Project administration. *Dimitrios Boubitsas:* Methodology, Investigation, Data analysis, Writing-Original Draft & Revision. *Liming Huang:* Methodology, Investigation, Data analysis, Writing-Original Draft, Writing-Revision & Editing.

**Declaration of competing interest**

We declare that there are no known competing financial interests or

personal relationships that could have appeared to influence the work reported in this paper.

**Data availability**

Data will be made available on request.

**Acknowledgement**

The authors wish to acknowledge the financial supports to this long-term study provided by Swedish Transport Administration and partly by Cementa AB. Special thanks are presented to Prof. Zareen Abbas at University of Gothenburg for his help in the Monte Carlo simulations for the ionic saturation indexes.

Appendix A

The chloride penetration profiles predicted by the modified ClinConc model for the other types of binders are shown in Figs. A1 to A4.

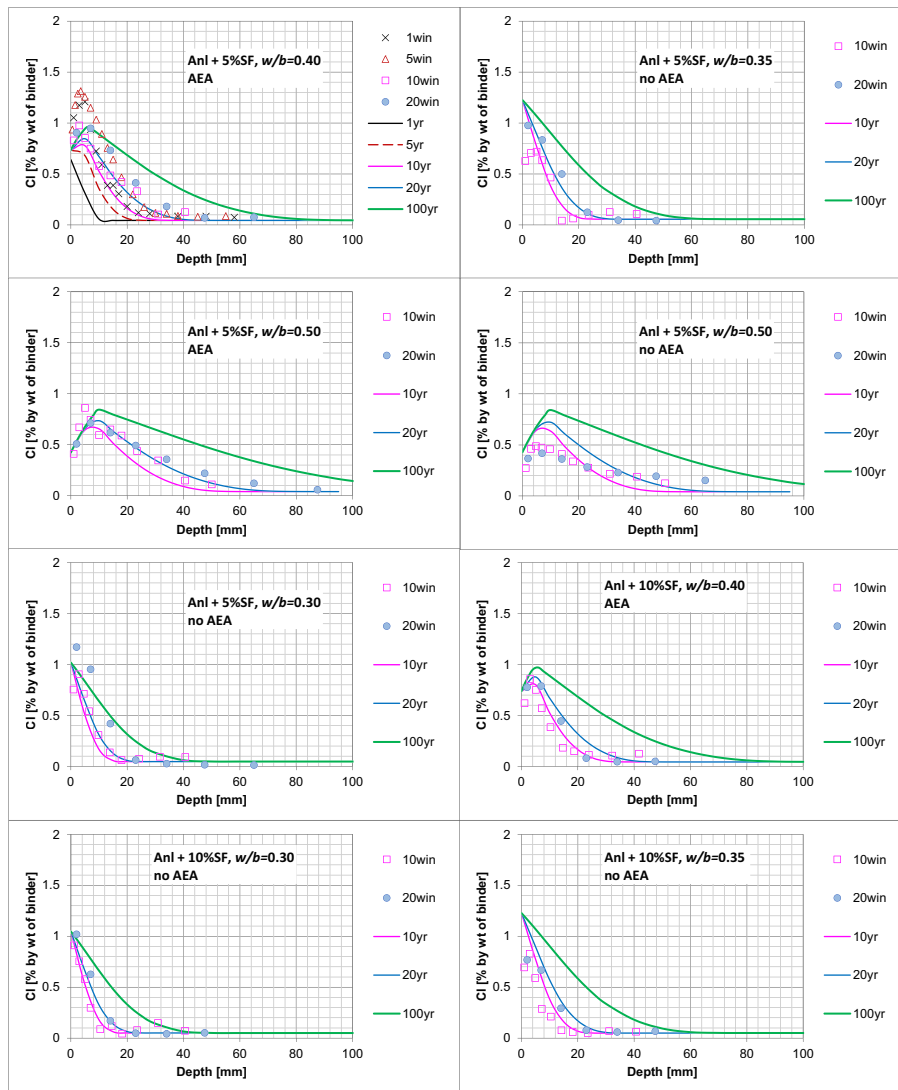


Fig. A1. Comparison of the measured (marks, win = winter) and predicted (lines, yr = year) chloride penetration profiles in concretes with the binder Anl + 5 %–10%SF.

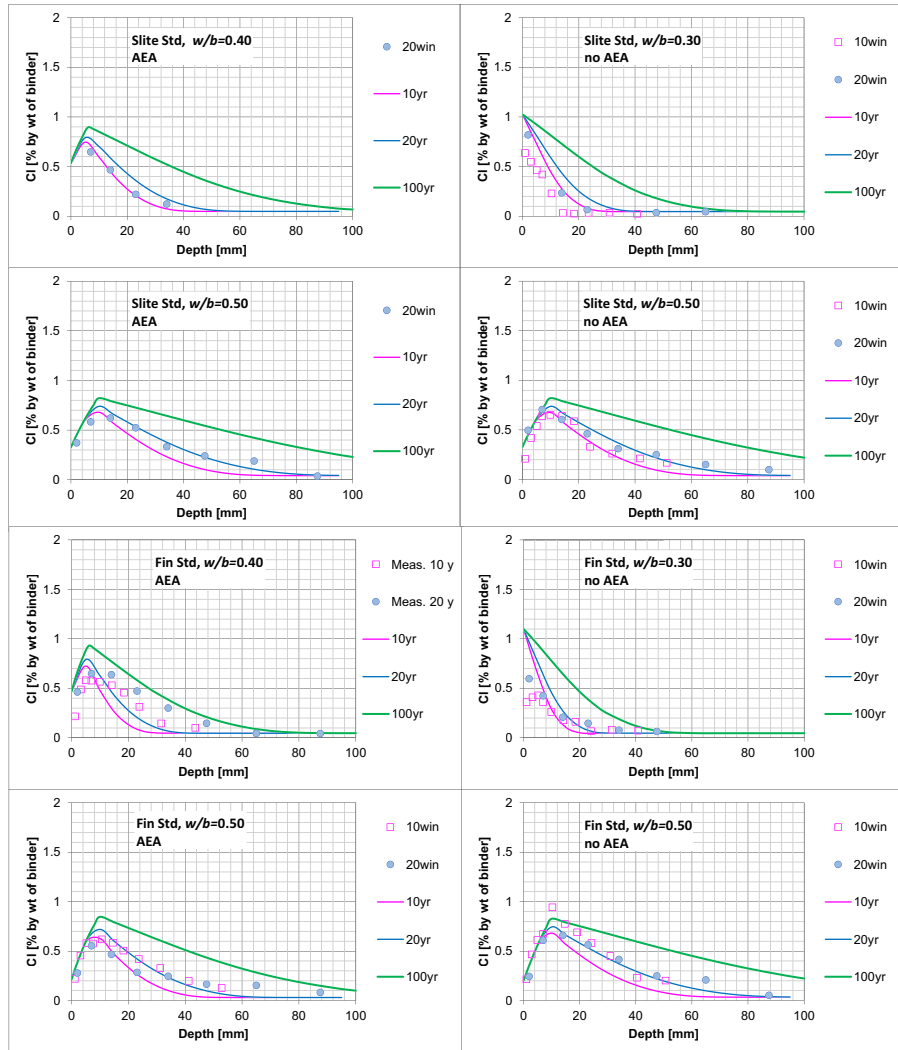


Fig. A2. Comparison of the measured (marks, win = winter) and predicted (lines, yr = year) chloride penetration profiles in concretes with the binders Slite Std and Fin Std.

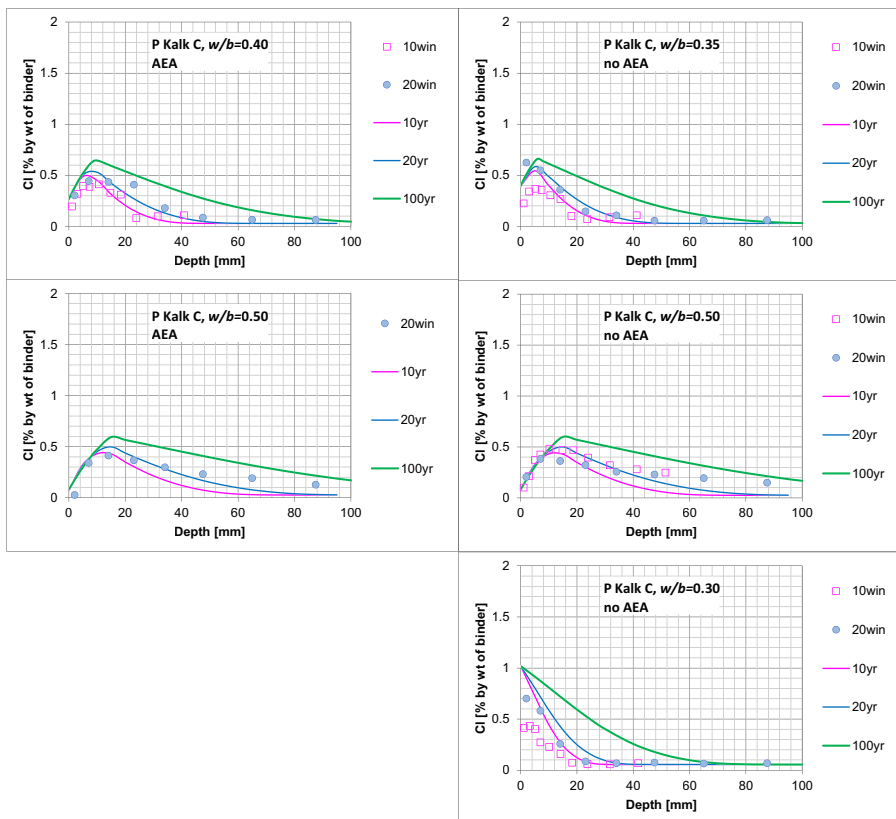


Fig. A3. Comparison of the measured (marks, win = winter) and predicted (lines, yr = year) chloride penetration profiles in concretes with the binder P Kalk C.

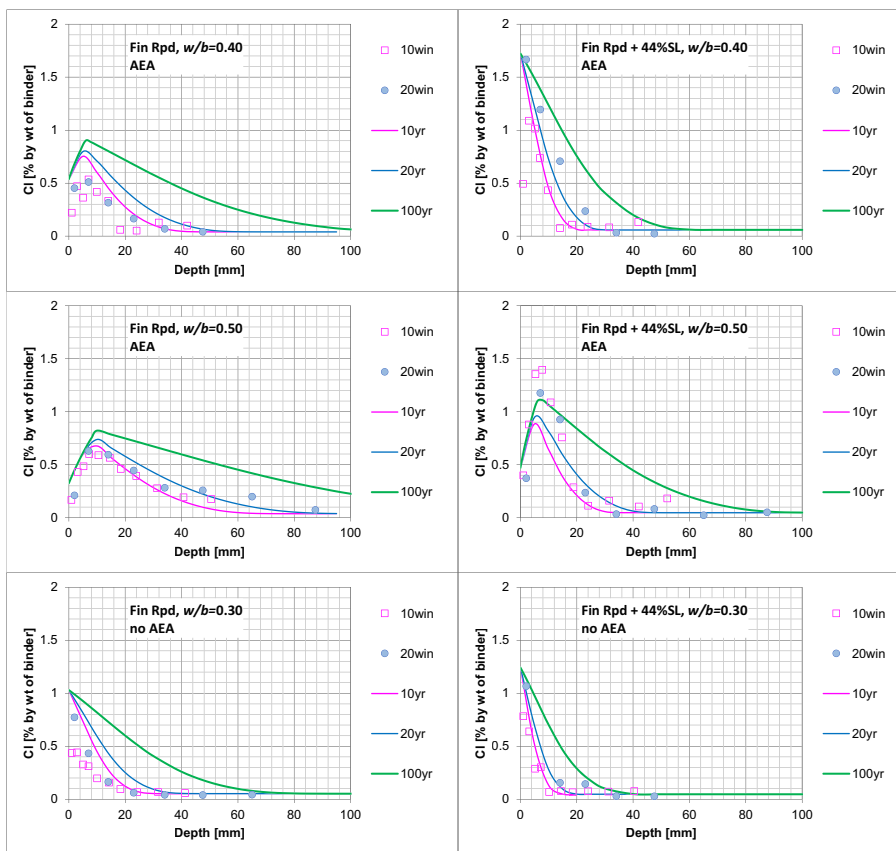


Fig. A4. Comparison of the measured (marks, win = winter) and predicted (lines, yr = year) chloride penetration profiles in concretes with the binders Fin Rpd and Fin Rpd + 44%SL.

**Table A1**  
Parameters applied in ClinConc model for simulation of chloride profile of concretes in Table 3.

Binder type	Binder kg/m <sup>3</sup>	$D_{RCM, 6m}$	Binding factor $f_b$	Binding exponent $\beta_b$	Time-dependent binding $a_t$	$k_D$	Age factor n	Gel quantity $W_{gel,6m}$ , kg/m <sup>3</sup>	Pore volume $V_{pore,6m}$	c [OH <sup>-</sup> ] mol/L
100%Anl	420	9.51	3.6	0.38	0.120	1	0.093	390.1	0.10	0.61
	380	21.42	3.6	0.38	0.073	1	0.066	404	0.12	0.44
	500	2.81	3.6	0.38	0.167	1	0.118	309.4	0.09	0.77
	450	4.36	3.6	0.38	0.143	1	0.105	351.2	0.10	0.65
	380	12.04	3.6	0.38	0.073	1	0.066	402.8	0.12	0.45
95%Anl + 5%SF	260	93.7	3.6	0.38	0.120	1	0.093	312.7	0.14	0.26
	420	3.78	3.6	0.38	0.127	1	0.096	384.5	0.11	0.56
	380	8.95	3.6	0.38	0.073	1	0.066	396.4	0.14	0.42
	500	1.12	3.6	0.38	0.173	1	0.121	309.3	0.11	0.70
	450	1.99	3.6	0.38	0.150	1	0.109	349.1	0.12	0.59
100%FinStd	380	7.58	3.6	0.38	0.073	1	0.066	398.4	0.14	0.40
	420	3.41	4.04	0.36	0.120	1	0.093	371.4	0.12	1.41
	380	7.4	4.04	0.36	0.073	1	0.066	383.6	0.15	1.06
100%SliteStd	540	1.81	4.04	0.36	0.167	1	0.118	317.8	0.12	1.84
	390	14.27	3.6	0.38	0.073	1	0.066	417.6	0.14	1.21
	420	6.82	3.6	0.38	0.120	1	0.093	391.6	0.10	1.33
56%FinRpd + 44%SL	390	14.8	3.6	0.38	0.073	1	0.066	416.8	0.13	0.97
	520	3.61	3.6	0.38	0.167	1	0.118	323.4	0.10	1.66
	410	14.27	3.6	0.38	0.073	1	0.066	438.1	0.14	0.97
100%Fin Rpd	420	1.5	5.16	0.32	0.120	1	0.093	322.4	0.18	0.95
	370	3.25	5.15	0.32	0.073	1	0.066	319.3	0.19	0.78
	540	0.79	5.15	0.32	0.167	1	0.118	277.9	0.17	1.24
90%Anl + 10%SF	420	6.82	3.6	0.38	0.120	1	0.093	392.4	0.11	1.89
	380	14.8	3.6	0.38	0.073	1	0.066	404	0.12	1.47
	540	3.61	3.6	0.38	0.167	1	0.118	335.5	0.11	2.43
P Kalk C	420	3.78	3.6	0.38	0.133	1	0.1	377.4	0.12	0.52
	500	1.12	3.6	0.38	0.180	1	0.124	311.6	0.13	0.60
	450	1.99	3.6	0.38	0.157	1	0.112	344.4	0.12	0.56
P Kalk C	420	6.82	3.6	0.38	0.120	1	0.093	392	0.11	1.18
	390	14.8	3.6	0.38	0.073	1	0.066	415.5	0.13	0.89
	530	3.61	3.6	0.38	0.167	1	0.118	328.3	0.10	1.55
	470	5.47	3.6	0.38	0.143	1	0.105	367.3	0.11	1.32
	400	14.27	3.6	0.38	0.073	1	0.066	428.3	0.14	0.85

## References

- [1] H. Beushausen, R. Torrent, M.G. Alexander, Performance-based approaches for concrete durability: state of the art and future research needs, *Cem. Concr. Res.* 119 (2019) 11–20, <https://doi.org/10.1016/j.cemconres.2019.01.003>.
- [2] K. Tuutti, Corrosion of steel in concrete, Swedish Cement and Concrete Research Institute (CBI), Stockholm, Sweden, 1982. <https://www.diva-portal.org/smash/get/diva2:960656/FULLTEXT01.pdf>.
- [3] P.-E. Petersson, Scaling resistance of concrete – testing according to SS 13 72 44, in: Freeze-Thaw and de-Icing Resistance of Concrete : Research Seminar Held in Lund, June 17, 1991, RILEM Committee TC-117 FDC, Division of Building Materials, LTH, Lund University, Lund, Sweden, 1991. <https://lucris.lub.lu.se/ws/files/4868047/1781975.pdf#page=101>.
- [4] L. Tang, P.-E. Petersson, Slab test: freeze/thaw resistance of concrete—internal deterioration, *Mater. Struct.* 37 (2004) 754–759.
- [5] G. Fagerlund, A service life model for internal frost damage in concrete, Division of Building Materials, LTH, Lund University, 2004. <https://lucris.lub.lu.se/ws/portalfiles/portal/4589573/1785152.pdf>.
- [6] G. Fagerlund, Moisture design with regard to durability: with special reference to frost destruction, Division of Building Materials, LTH, Lund University, Lund, Sweden, 2006. <https://lucris.lub.lu.se/ws/portalfiles/portal/4701334/1515012.pdf>.
- [7] P.-E. Petersson, A service life model for scaling resistance of concrete—reflections, in: Meeting of the Fib Task Group, Lund, Sweden, 2004.
- [8] L. Tang, L.-O. Nilsson, Rapid determination of the chloride diffusivity in concrete by applying an electric field, *ACI Mater. J.* 89 (1993) 49–53.
- [9] L. Tang, Chloride Transport in Concrete-measurement and Prediction, Chalmers University of Technology, Sweden, 1996. Doctor Thesis.
- [10] L. Tang, Engineering expression of the ClinConc model for prediction of free and total chloride ingress in submerged marine concrete, *Cem. Concr. Res.* 38 (2008) 1092–1097.
- [11] P. Utgenannt, The influence of ageing on the salt-frost resistance of concrete, PhD Thesis, Division of Building Materials, LTH, Lund University, 2004. <https://lup.lub.lu.se/search/files/4399727/1480972.pdf>.
- [12] K. Fridh, Internal frost damage in concrete-experimental studies of destruction mechanisms, PhD Thesis, Division of Building Materials, LTH, Lund University, 2005. <https://lucris.lub.lu.se/ws/portalfiles/portal/4697606/1480966.pdf>.
- [13] L. Tang, P. Utgenannt, Chloride ingress and reinforcement corrosion in concrete under de-icing highway environment—a study after 10 years' field exposure, Sp Technical Research Institute of Sweden, Borås, Sweden, 2007. <https://www.diva-portal.org/smash/get/diva2:962438/FULLTEXT01.pdf>.
- [14] L. Bo, Chloride Transport in Concrete Under the Frost Action—An Experimental Study, Department of Civil and Environmental Engineering, Chalmers University of Technology, 2009. Licentiate Thesis.
- [15] L. Tang, P. Utgenannt, Validation of models and test methods for assessment of durability of concrete structures in the road environment, CBI Swedish Cement and Concrete Research Institute, Stockholm, Sweden, 2012. <https://www.diva-portal.org/smash/record.jsf?dswid=-6937&pid=diva2%3A960650>.
- [16] D. Boubitsas, L. Tang, P. Utgenannt, Chloride Ingress in Concrete Exposed to Marine Environment-field Data up to 20 Years' Exposure, Borås, Sweden, 2014.
- [17] B.P. Rob, H. Angelica, Penetration of chloride from de-icing salt into concrete from, *Heron* 45 (2000) 2.
- [18] G. Kristaps, P. Ainars, Concrete bridge deterioration caused by de-icing salts in high traffic volume road environment in Latvia, Balt. J. Road Bridg. Eng. 9 (2014) 200–207, <https://doi.org/10.3846/bjrbe.2014.25>.
- [19] M. Xie, P. Dangla, K. Li, Reactive transport modelling of concrete subject to de-icing salts and atmospheric carbonation, *Mater. Struct.* 54 (2021) 240, <https://doi.org/10.1617/s11527-021-01835-2>.
- [20] Z.-H. Lu, Y.-G. Zhao, Z.-W. Yu, F.-X. Ding, Probabilistic evaluation of initiation time in RC bridge beams with load-induced cracks exposed to de-icing salts, *Cem. Concr. Res.* 41 (2011) 365–372, <https://doi.org/10.1016/j.cemconres.2010.12.003>.
- [21] P. Utgenannt, Main Area 1 – Reinforcement Corrosion, Salt and Moisture Transport: Samples Manufactured in 1990 – Material and Manufacturing Data and Results From Resistance Testing in the Laboratory, SP Sveriges Provnings- och forskningsinstitut, Borås, Sweden, 1998.
- [22] D. Boubitsas, L. Tang, K. Fridh, U. Müller, P. Utgenannt, Frost resistance of concrete—experience from long-term field exposure, RISE - Research Institutes of Sweden, Samhällsbyggnad, CBI Betonginstitutet, 2018. <https://www.diva-portal.org/smash/get/diva2:1282289/FULLTEXT01.pdf>.
- [23] K. Nordström, A. Andersen, S. Backe, T. Lundgren, P. Utgenannt, Manual of specimens deployed at RV 40: beams manufactured in 1996 - specimens with decoration and molded-in measuring equipment, Lund Tekniska Högskola, Byggnadsmaterial, Lund, Sweden, 1998. <https://lucris.lub.lu.se/ws/portalfiles/portal/4377207/4388391.pdf>.

- [24] K. Fridh, Manual of Specimens Deployed at RV 40: Beam Fabricated 1996 Specimens with Arming and Cast-in Gauges, Lund Tekniska Högskola, Byggnadsmaterial, Lund, Sweden, 1998.
- [25] L. Tang, Mapping corrosion of steel in reinforced concrete structures, SP Swedish National Testing and Research Institute, Borås, Sweden, 2002. <https://www.diva-portal.org/smash/get/diva2:962223/FULLTEXT01.pdf>.
- [26] D. Boubitsas, L. Tang, The influence of reinforcement steel surface condition on initiation of chloride induced corrosion, *Mater. Struct.* 48 (2015) 2641–2658.
- [27] O.M. Jensen, P.F. Hansen, Water-entrained cement-based materials I. Principles and theoretical background, *Cem. Concr. Res.* 34 (2001) 647–654.
- [28] M.H.N. Yio, H.S. Wong, N.R. Buenfeld, 3D pore structure and mass transport properties of blended cementitious materials, *Cem. Concr. Res.* 117 (2019) 23–37, <https://doi.org/10.1016/j.cemconres.2018.12.007>.
- [29] L. Huang, L. Tang, I. Löfgren, N. Olsson, Z. Yang, Real-time monitoring the electrical properties of pastes to map the hydration induced microstructure change in cement-based materials, *Cem. Concr. Compos.* 132 (2022), 104639, <https://doi.org/10.1016/j.cemconcomp.2022.104639>.
- [30] L. Huang, L. Tang, I. Löfgren, N. Olsson, Z. Yang, Y. Li, Moisture and ion transport properties in blended pastes and their relation to the refined pore structure, *Cem. Concr. Res.* 161 (2022), 106949, <https://doi.org/10.1016/j.cemconres.2022.106949>.
- [31] B. Martín-Pérez, H. Zibara, R.D. Hooton, M.D.A. Thomas, A study of the effect of chloride binding on service life predictions, *Cem. Concr. Res.* 30 (2000) 1215–1223, [https://doi.org/10.1016/S0008-8846\(00\)00339-2](https://doi.org/10.1016/S0008-8846(00)00339-2).
- [32] R. Luo, Y. Cai, C. Wang, X. Huang, Study of chloride binding and diffusion in GGBS concrete, *Cem. Concr. Res.* 7 (2003).
- [33] A. Machner, M.H. Bjørndal, H. Justnes, L. Hanžič, A. Šajna, Y. Gu, B. Bary, M. Ben Haha, M.R. Geiker, K. De Weerd, Effect of leaching on the composition of hydration phases during chloride exposure of mortar, *Cem. Concr. Res.* 153 (2022), 106691, <https://doi.org/10.1016/j.cemconres.2021.106691>.
- [34] A. Machner, M. Bjørndal, A. Šajna, N. Mikanovic, K. De Weerd, Impact of leaching on chloride ingress profiles in concrete, *Mater. Struct.* 55 (2022) 8, <https://doi.org/10.1617/s11527-021-01730-w>.
- [35] P. Hemstad, A. Machner, K. De Weerd, The effect of artificial leaching with HCl on chloride binding in ordinary Portland cement paste, *Cem. Concr. Res.* 130 (2020), 105976, <https://doi.org/10.1016/j.cemconres.2020.105976>.
- [36] N. Olsson, B. Lothenbach, V. Baroghel-Bouny, L.-O. Nilsson, Unsaturated ion diffusion in cementitious materials – the effect of slag and silica fume, *Cem. Concr. Res.* 108 (2018) 31–37, <https://doi.org/10.1016/j.cemconres.2018.03.007>.
- [37] S. Fjendbo, H.E. Sørensen, K. De Weerd, U.H. Jakobsen, M.R. Geiker, Correlating the development of chloride profiles and microstructural changes in marine concrete up to ten years, *Cem. Concr. Compos.* 131 (2022), 104590, <https://doi.org/10.1016/j.cemconcomp.2022.104590>.
- [38] D. Boubitsas, L. Tang, The influence of reinforcement steel surface condition on initiation of chloride induced corrosion, *Mater. Struct.* 48 (2015) 2641–2658.
- [39] Z.H. Zou, J. Wu, Z. Wang, Z. Wang, Relationship between half-cell potential and corrosion level of rebar in concrete, *Corros. Eng. Sci. Technol.* 51 (2016) 588–595.
- [40] L. Tang, P. Utgenannt, D. Boubitsas, Durability and service life prediction of reinforced concrete structures, *J. Chin. Ceram. Soc.* 43 (2015) 1408–1419.
- [41] J. Liu, W. Zhang, Z. Li, H. Jin, L. Tang, Influence of deicing salt on the surface properties of concrete specimens after 20 years, *Constr. Build. Mater.* 295 (2021), 123643, <https://doi.org/10.1016/j.conbuildmat.2021.123643>.
- [42] J. Kim, W.J. McCarter, B. Suryanto, S. Nanukuttan, P.A.M. Basheer, T.M. Chrisp, Chloride ingress into marine exposed concrete: a comparison of empirical- and physically- based models, *Cem. Concr. Compos.* 72 (2016) 133–145, <https://doi.org/10.1016/j.cemconcomp.2016.06.002>.
- [43] L. Tang, Chloride penetration profiles and diffusivity in concrete under different exposure conditions, Department of Building Materials, Chalmers University of Technology, Gothenburg, Sweden, 1997. <https://research.chalmers.se/publication/23503>.
- [44] L. Tang, I. Löfgren, Evaluation of durability of concrete with mineral additions with regard to chloride-induced corrosion, Division of Building Technology, Chalmers Universities of Technology, Gothenburg, Sweden, 2016. [https://publications.lib.chalmers.se/records/fulltext/241518/local\\_241518.pdf](https://publications.lib.chalmers.se/records/fulltext/241518/local_241518.pdf).
- [45] K. Hong, R.D. Hooton, Effects of cyclic chloride exposure on penetration of concrete cover, *Cem. Concr. Res.* 29 (1999) 1379–1386.
- [46] P. Castro, O.T. De Rincon, E.J. Pazini, Interpretation of chloride profiles from concrete exposed to tropical marine environments, *Cem. Concr. Res.* 31 (2001) 529–537.
- [47] C. Arya, P. Vassie, S. Bioubakhsh, Modelling chloride penetration in concrete subjected to cyclic wetting and drying, *Mag. Concr. Res.* 66 (2014) 364–376.
- [48] J. Liu, Q. Qiu, X. Chen, F. Xing, N. Han, Y. He, Y. Ma, Understanding the interacted mechanism between carbonation and chloride aerosol attack in ordinary Portland cement concrete, *Cem. Concr. Res.* 95 (2017) 217–225, <https://doi.org/10.1016/j.cemconres.2017.02.032>.
- [49] K. Li, F. Zhao, Y. Zhang, Influence of carbonation on the chloride ingress into concrete: theoretical analysis and application to durability design, *Cem. Concr. Res.* 123 (2019), 105788, <https://doi.org/10.1016/j.cemconres.2019.105788>.
- [50] K. De Weerd, G. Plusquellec, A. Belda Revert, M.R. Geiker, B. Lothenbach, Effect of carbonation on the pore solution of mortar, *Cem. Concr. Res.* 118 (2019) 38–56, <https://doi.org/10.1016/j.cemconres.2019.02.004>.
- [51] A.K. Suryavanshi, R. Narayan Swamy, Stability of Friedel's salt in carbonated concrete structural elements, *Cem. Concr. Res.* 26 (1996) 729–741, [https://doi.org/10.1016/S0008-8846\(96\)85010-1](https://doi.org/10.1016/S0008-8846(96)85010-1).
- [52] O.A. Kayyali, M.N. Haque, Effect of carbonation on the chloride concentration in pore solution of mortars with and without flyash, *Cem. Concr. Res.* 18 (1988) 636–648.
- [53] H. Chang, S. Mu, D. Xie, P. Wang, Influence of pore structure and moisture distribution on chloride "maximum phenomenon" in surface layer of specimens exposed to cyclic drying-wetting condition, *Constr. Build. Mater.* 131 (2017) 16–30, <https://doi.org/10.1016/j.conbuildmat.2016.11.071>.